University ABBES LAGHROUR Khenchela
Faculty of Science and Technology
Department of Industrial Engineering
جامـــعة عبـــاس لـــــغرور خـنـشـلة
كليـــة العلـــوم والتكنـــولـــوجيـا
قسم الهنـدسة الصنـاعية

Serial N° :.....

Final year project report

For obtaining the Master's degree

Sector: Electrotechnics

Specialty: Electrical Controls

Presented by

Adjeroudi Akram

&

Aghrou Mouna

THEME

Control of a quadcopter in perturbed environment

Supported on: *before the examination committee composed of:*

Tarek Boutaba	***Dr***	***at Abbes Laghrour University of Khenchela***	***President***
Mokhtari Khalil	***Dr***	***at Abbes Laghrour University of Khenchela***	***Supervisor***
Saidi	***Dr***	***at Abbes Laghrour University of Khenchela***	***Examiner***

Promotion 2022/2023

Dedication

Adjeroudi Akram,

I dedicate this humble work to our dear parents, who have been a constant source of support and encouragement throughout our academic journey. Without their unwavering assistance, we would not have been able to successfully complete this thesis and achieve my goals.

I would like to express my heartfelt gratitude to my brothers Ousama, Imad, Moncef, and my dear sister Ritej, as well as our entire family. Your unwavering support and belief in me have been a driving force behind my accomplishments. I hope that I can continue to make you all proud in the future.

I would like to extend my heartfelt dedication to my English teacher, Mr. Nabil Hantach, and my brother Imad for their invaluable support and assistance in the field of English. Their guidance and encouragement have greatly contributed to my language skills in Polyglot academy.

I would also like to express my gratitude to my dear friends, Diaa Eldine Djaarir, Ounissi Ghylas, Balouli Marwan, Balouli Amine, Mezahdia Aymen, Gasmi Ziad, Aissaoui Radhwan, specially home and all of my beloved people. Your friendship and unwavering support have been a constant source of inspiration and motivation throughout my journey. thank you for being with me till that moment.

Aghrou Mouna,

Praise be to God, that is enough, and prayers be upon the beloved Chosen One, his family, and those who have fulfilled their faith. As for what follows: Praise be to God, who has enabled us to value this step in our academic journey with our memorandum. I dedicate the fruit of my success and effort to all the honorable family who supported me and still do, and to the companions of the journey who shared its moments with me, may God bless and grant them success.

Acknowledgements

We would like to express my gratitude to God Almighty for giving us the courage, patience, willpower, and strength to face all the difficulties and obstacles that have come our way throughout our years of study.

We extend our sincere thanks to all our teachers at the University of Abbes Laghror Khenchela, especially our supervisor Mr. Khalil Mokhtari, for proposing the topic on which We worked and for providing guidance and support throughout the preparation of this thesis.

We would also like to express our appreciation to Mr. Bediaf Yacine for generously sharing his experience, knowledge and ideas, which greatly contributed to the completion of study years.

We am particularly grateful to the members of the examination committee for their interest in this work.

This page would not be complete without acknowledging our parents and specially .Without their support, we would not have been able to successfully complete this thesis.

Lastly, our thanks go to all those who supported us, near or far, in achieving this work.

With our sincere regards.

Résumé

Ce mémoire se concentre sur le dévélopement de techniques de commandes pour but de stabiliser un systéme de type quadricoptère dans un environement perturbé.

Le modèle dynamique du quadricoptère est établi en utilisant le formalisme de Newton-Euler, le caractérisant comme un système sous-actionné avec une complexité, une non-linéarité et des états interdépendants.

Deux structures de contrôle, le contrôle PID et le contrôle synergetique, sont introduites et comparées.Une tell comparaison vise à évaluer leurs performances dans le contrôle du quadricoptère en présence de perturbation externes.

Une validation expérimentale pour confirmer les résultats théoriques a été établie a l'aide d'un banc d'essai quadrirotor.

Abstract

This thesis focuses on the development of control techniques aiming to stabilize a quadcopter system in a disturbed environment.

The dynamic model of the quadcopter is established using the Newton-Euler formalism, characterizing it as an underactuated system with complexity, nonlinearity, and interdependent states.

Two control structures, PID control and synergetic control, are introduced and compared. Such a comparison aims to evaluate their performances in controlling the quadcopter in the presence of external disturbances.

Experimental validation to confirm the theoretical results has been conducted using a quadcopter test bench.

Contents

List of Figures

List of tables

Nomenclature

Notations

$\mathbb{F}$	Denote the field of real numbers.
Ω	Rotational speed in the fixed frame of reference.
v	Linear velocity in the fixed frame of reference.
$\mathbb{R}$	Rotation matrix.
$\mathbb{T}$	Transformation matrix.
ε	Position vector.
ϕ	Roll angle.
θ	Pitch angle.
ψ	Yaw angle.
ω	Engine rotation speed.
ω_d	Desired motor rotation speed.
ω	Error between ω and ω_d.
τ	Input torque of the motors.
u	The control signal.
x	State variable
x_d	Desired state.
e	Tracking error.
t	Time variable.
V	Lyapunov function.
y	Output variable.
y_r	Desired trajectory.
d_θ	Disturbance on the pitch angle.
d_ϕ	Disturbance on the roll angle.
d_ψ	Disturbance on the yaw angle.

Acronyms / Abbreviations

UAV	Unmanned Aerial Vehicles.
VTOL	Vertical Take off and Landing.
PID	Proportional integral derivative.
DoF	Degree of freedom.

General Introduction

Modern industrial systems increasingly rely on advanced control techniques with the aim of achieving high levels of performance. However, if a fault occurs in a system, these control strategies can prove to be very limited, leading to undesired behaviors and even instability, especially in critical systems such as nuclear power plants and aircraft.

With the democratization and increased accessibility of drones, these devices are being used in a wide range of fields. Examples include traffic monitoring, environmental exploration, aerial mapping and photography, not to mention various military applications. The quadrotor drones' ability to take off and land vertically, their agility, and their capability for hovering make them highly versatile devices with utility limited only by imagination [**?**].

During flight, quadrotors are subject to various disturbances, which can be either exogenous or endogenous. Exogenous disturbances are caused by atmospheric conditions, while endogenous disturbances arise from the internal state of the drone. These disturbances make the modeling process tedious and challenging.

The design of drones is essentially divided into two parts: the control part and the hardware part. Despite the challenges associated with this work, researchers and designers have been heavily involved in both activities to make contributions in this field. The algorithmic part focuses on the development of control laws. Control engineers are increasingly interested in studying and developing both linear and nonlinear control laws to govern the dynamics of these vehicles. The second part involves the development of the experimental platform or autopilot that will be embedded in the vehicle.

The objective of this work is to build a quadrotor drone controlled through flight command (remote control). This thesis is structured around four chapters:

- Chapter 1: In this chapter, we will present general information about drones. Its purpose is to explain what drones are, demonstrate their considerable potential, and introduce the most basic concepts.
- Chapter 2: This chapter is dedicated to the dynamic modeling of the quadrotor. Firstly, we provide a description of the system from a general structural perspective. Then, we highlight the dynamic modeling of the quadrotor using the Newton-Euler formalism. Open-loop simulation results are provided to show the inherent stability of the Quadcopter.

- Chapter 3: In this chapter, we delve into the theoretical foundations of two control techniques. The first technique is the PID controller, and the second technique is the synergetic controller. We also explore the application of these control laws to the quadrotor. Numerical simulation studies are given in order to highlight the performances of the proposed controllers.
- Chapter 4: This final chapter focuses on the experimental validation of the synergetic control using a quadrotor test bench.

Chapter 1

General information about drones

1.1 Introduction

Drones are aerial vehicles equipped with cameras, sensors, communication devices, and other equipment. They are utilized for various purposes, including reconnaissance missions, data collection, and even military operations. In this chapter, we provide a comprehensive overview of drones, covering their historical background and classifications. We then focus on the quadcopter configuration, which is the main focus of our study, discussing its advantages, evolutionary advancements, technological aspects, and application areas.

1.2 History

Man has always been fascinated by the flight of birds and the conquest of the skies, this wonder has fed many myths and legends like the dream of Icarus. However, although it is equipped with wings repeating the sinusoidal movement by beating it could invent the wheel, at the base of which any movement became possible. It turns out that they were the Chinese, 400 years before J-C3; who were the first to invent a toy that rose by rotating it rapidly between the hands, called a "Chinese spinning top" illustrated in Figure 1.1. As early as 1480, Leonardo da Vinci had drawn a figure 1.2 machine, a kind of aerial screw, whose sail turned around a vertical axis . Borrelli, in 1680, and Paucton, in 1768, resumed the study of these theories.

In 1754, the Russian Lomonossov tested before a scientific assembly a complex model with two counter-rotating coaxial rotors, moved by a clockwork mechanism, and demonstrated the existence of a lifting force. On April 28, 1784 when the naturalist Launoy and the physicist Bienvenu produced before the Academy of Sciences a reduced model with two counter-rotating propellers, moved by an arc spring mechanism, a discovery taken up in 1795 by George Cayley.

In 1849 bombardments on Venice took place, from the Vulcano, by means of unmanned balloons equipped with time bombs. In 1862, the French Ponton d'Amécourt, to whom we owe the word "helicopter" and in 1877, the Italian Forlanini built devices, powered by steam engines. Ten years later, the Frenchman Trouve took off with a model equipped with an electric motor, whose power supply is obtained from the ground by fine copper wires.

In 1898, Nikola Tesla was the first to develop the concept of a remotely controlled flying machine, he demonstrated it with what called it "tele-automation". Tesla passed on his idea to Peter Cooper Heweit, who passed it on to Elmer Sperry, the latter establishing the field of unmanned aviation. It was in 1907, a week before Paul Cornu's helicopter, that the world's first real helicopter take-off was successful. Louis Breguet and Charles Richet succeed in hovering at 50 cm from the ground with a vertical take-off flying machine of their invention called the "gyroplane", this is a Quadcopter powered by a gasoline engine, this flight was so unstable that four men were needed to hold the machine.

[2] [3] In 1914, Sperry's son publicly demonstrated automatic aircraft stabilization. 2 years later, in 1916, in the United States, aerial vehicles were born with the AerialTarget, a target aircraft, a number of improvements followed during and after the First World War, radio-controlled unmanned aircraft were born , with aerial torpedo attempts remotely controlled by wireless telegraphy waves and carrying a gyroscope. The first French drone was designed, produced and tested in 1923 in Etampes by engineer Maurice Percheron and Captain Max Boucher; but the French army did not then find any interest in this new technology.

The next phase in the 1930s was the use of autonomous target aircraft in both the United Kingdom and the United States of America where the Radioplane OQ-2, a small remotely piloted aircraft, was mass-produced. From 1938 the German army developed remotely guided vectors in the form of hovering anti-ship bombs, radio-guided anti-tank bombs and wire-guided tracked vehicles.

The great development of drones dates from the wars in Korea and Vietnam. At this time of the Cold War, the drone was developed in a confidential way by the United States of America as a means of strategic superiority and capacity rupture intended to allow surveillance and military intervention in the enemy without incurring the human risks that public opinion did not support it. This superiority has been acquired through technological innovation, especially in the areas of automatics and transmissions.

The transfers to The Zionist entity of certain systems have enabled this country to pragmatically develop a collection of short and medium range tactical drones with direct data transmissions. Drones were then used in all conflicts and peacekeeping operations. It has notably been used in Kosovo or Chad, during American air attacks in Pakistan or against maritime piracy, by the Americans who introduced it in 2009 [2].

1.3 Classification of drones

The classification of aerial systems is difficult, because there are many types of aerial drones starting from the nano drone of a few grams to the heavy drone capable of carrying out missions of more than 24 hours at several thousand kilometers from its base. However, autonomous vehicles can be classified into several categories according to: cruising altitude, range, endurance, size (length, wingspan, etc.) or even their wing [4] [5].

1.3.1 Classification according to size

1.3.1.1 HALE (High Altitude Long Endurance)

These are large drones, most often fixed-wing. They are able to stay in flight for a very long time and collect information over very long periods (12 to 48 hours). Such as the Global Hawk (Northrop Gumman), the size of an airliner and flying at altitudes of up to 20 km with a range of several thousand kilometres. Combat drones (UCAV Unmanned Combat Air Vehicles), such as the Neuron (Boeing), designed for attack missions. Tactical drones, such as the Sperwer (SAGEM) or the Aerostar (AeronauticsDefense Systems), used for reconnaissance or battlefield supervision missions and flying at an altitude of between 200m and 5km, for a range of 30 at 500km [2] [5].

Figure 1.1: High Altitude Long Endurance

1.3.1.2 MALE (Medium Altitude Language Endurance)

They are used for long duration flights at medium operational altitude, with a long range. Such as the Eagle 1 (EADS) or the Predator (General Atomics), with a wingspan of the order of ten meters and flying at altitudes between 5km and 12km for a range of up to 1000km.

[2] [4]

Figure 1.2: Medium Altitude Long Endurance

1.3.1.3 Mini drones

They are rather light and small drones (up to a few kilograms and with a wingspan of up to 1 to 2 meters) facilitating the implementation of a relatively low autonomy (10 to 30 minutes) and generally used for observation hard-to-reach areas. Such as the Hovereye (Bertin Technologies) or the Dragon Eye (AeroVironment) whose maximum size does not exceed one meter. [2]

Figure 1.3: mini drone

1.3.1.4 Micro drones

These are drones with varying sizes from a centimeter to a few tens of centimeters,usually electrically powered. Thus, they allow fly indoors,such as the PicoFlyer (Proxyflyer), whose dimension maximum does not exceed 15 cm. [2] [4]

Figure 1.4: Micro drone

1.3.2 Classification according to mode of propulsion

Aerodynamic operation provides another possibility of classification. Thereby, drones can be structured into three families:

1.3.2.1 Fixed-wing drones

These drones are capable of various modes of displacement, including:

1. Heavier than air: aircraft type.
2. Lighter than air: A type of airship that uses helium to generate vertical thrust and rotors to generate torques. having a volume importantly, it moves slowly and is relatively more sensitive to the wind. [5]

Figure 1.5: Fixed-wing drone

1.3.2.2 Swing-wing drones

Swing-wing drones are versatile UAVs with wings that can change their sweep angle during flight. They offer enhanced lift and stability at lower speeds when the wings are fully extended. When the wings are swept back, the drones gain increased speed and maneuverability. This flexibility allows them to adapt to different operational requirements. Swing-wing drones are used for surveillance, reconnaissance, mapping, and military operations. However, their complexity and added weight can affect overall performance. Carefully designed control systems are necessary for safe operation. Overall, swing-wing drones provide optimal performance across different flight regimes, making them suitable for applications that require versatility and adaptability.

1.3.2.3 Rotary wing drones

This type is subdivided into several sub-classes:

- Configuration with a single rotor: In this configuration we find basically the planes called 3D. These planes have a single engine like main actuator, powerful enough to take off vertically and ailerons of a large surface area to ensure sufficiently large control torques so that the device be easy to drive. They develop more and more and they have the advantage of being able to fly like an airplane normal, which gives the possibility of moving quickly and very economically in terms of energy.
- Configuration Having two rotors: In this type of configuration we can distinguish between those that use one or two swashplates and those that use blades fixed pitch. Among those who use swashplates we have the helicopter classic with a main rotor and a que rotor. In this category you can also mention the tandem helicopter which has two rotors which turn in the opposite direction but in different axes. With regard to devices without swashplates, it is clear that with only two rotors one cannot generate a force and three independent torques. It is therefore necessary to add either fins or mechanisms to rotate the rotors.
- Configuration Having three rotors: In this category, we have the tricopter, vectron, and freestanding helicopter. The tricopter has two front rotors rotating in opposite directions, while the vectron has three rotors rotating in the same direction. The freestanding helicopter features two fixed-pitch rotors on the same axis, with a small tail rotor for pitch control. These drones offer different flight characteristics and stability properties, with the tricopter providing satisfactory performance. The self-stabilizing helicopter is designed for indoor use, ensuring stability through rotor blade articulation.
- Configuration Having four rotors: The Quadcopter is an aircraft lifted and propelled by four rotors located at the ends of a reinforcement. Its movement is controlled by adjusting the speed of each rotor to manipulate lift force and torque. Two rotors on the same axis rotate clockwise, while the other two rotate counterclockwise to counteract

torque. In ideal conditions, with identical components and balanced mass, the quadcopter achieves stable hovering flight on all three axes. An alternative configuration, known as X4, involves all rotors spinning in the same direction or two rotors inclined to create yaw torque, allowing control of rotation around the Z axis.

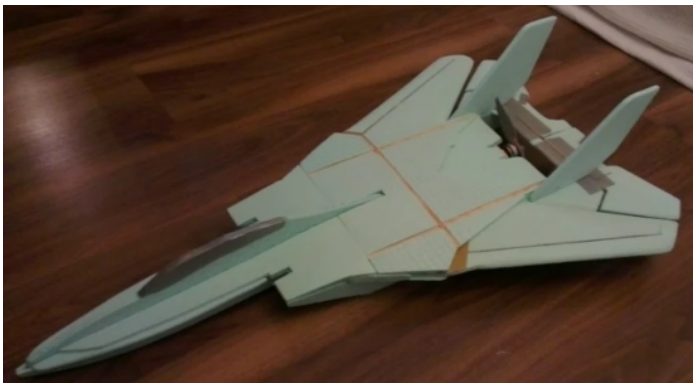

Figure 1.6: Swing-wing drone

1.4 The Quadcopter

1.4.1 Description

The quadrirotor is a flying object which has the particularity of having 4 rotors placed at the ends of a rigid body in the shape of a cross. The control electronics are generally placed in the center of the cross which constitutes the center of gravity of the machine. To prevent the Quadcopter from turning on itself around its yaw axis, the propellers belonging to the front-rear motor pair must turn in one direction and the propellers belonging to the left-right pair must turn in another direction. The Quadcopter being a completely unstable configuration, it is necessary to develop algorithms allowing to control each motor separately to counter the inclination on each axis and thus stabilize it.

1.4.2 Technology

Before ordering any system, it is necessary to define these components to be able to model it well, like any other robot, the quadrirotor consists essentially of a mechanical part which constitutes its skeleton and its muscles, plus an electronic part bringing together the sensors, the computer and communication modules.

1.4.3 Advantages of the quadcopter configuration

Quadcopter design offers real advantages over other configurations:

1. Their small size and their maneuverability allow them to fly in closed (Indoor) or open (Outdoor) environments and near obstacles opposed to conventional helicopters.
2. The simplicity of its mechanics facilitates its maintenance.-No clutch is required between the motor and the rotor and no requirement is given on the angle of attack of the rotors.
3. Four small rotors replace the large rotor of the helicopter which greatly reduces the stored kinetic energy and minimizes damage in the event of accidents.
4. Its vertical take-off and landing.
5. This configuration is controlled by only varying the rotation speed of the four motors.
6. Their lift capacity due to presence of four rotors instead of one which can be increased by lengthening the blades of a rotor or by increasing their number, but due to aerodynamic phenomena and size, this has its limits.
7. Reduction of the gyroscopic effect.
8. Its dynamics are weaker than those of the helicopter which does not require a fast reaction time.
9. Despite its four rotors and its stationary balance, the X4 remains an underactuated and dynamically unstable system. which results in the fact that a large percentage of the lift gained is used to lift the weight of the vehicle itself.
10. Their technology remains emerging, which does not encourage manufacturers to invest in it.

1.4.4 Application

1.4.4.1 Military applications

Quadcopters are widely utilized in military operations due to their compact size, agility, and suitability for navigating complex environments. Their vertical takeoff and landing capabilities enable deployment in diverse terrains without the need for runways. Equipped with various payloads, including cameras and sensors, Quadcopters enhance reconnaissance capabilities and provide real-time situational awareness. Their autonomous or remotely piloted operation reduces human exposure in high-risk missions, improving the safety of military personnel.

1.4.4.2 Civil applications

The civilian sector is progressively assuming various surveillance and operational roles where human presence is not necessary, and cost-effective operations are crucial. These missions

encompass tasks such as monitoring and managing shipping routes, addressing issues like illegal immigration, as well as detecting and mitigating pollution incidents. The following are some of the applications:

1. Surveillance of oil pipelines, gas pipelines, high voltage lines.
2. civil security missions (surveillance of road traffic, demonstrations, protection of reserved or prohibited areas, assessment of natural disasters such as forest fires, volcanic activity, etc.).
3. Inspection of works of art such as bridges, viaducts and dams.
4. Agricultural spreading, monitoring of cultivated areas and atmospheric measurements. For example, the "Deep Water" program for the American Coast Guard aims to acquire 76 drones for monitoring and take up new security challenges: Observation of oil and gas pipelines, surveillance of dangerous cargoes, detection of contraband thefts, acts of maritime piracy but also of water sources, archaeological remains, seams of raw materials or combustible [2] [6].

1.5 Conclusion

In conclusion, this chapter provides an overview of drones and Quadcopters, highlighting their significance in various fields. The chapter begins with a general introduction to drones, discussing their evolution, classifications, and potential applications. It then delves into the specific advantages and applications of Quadcopters, showcasing their versatility, maneuverability, and vertical takeoff and landing capabilities. Additionally, the chapter explores the historical development of Quadcopters, tracing their origins and highlighting notable advancements in their design and technology. This comprehensive exploration sets the foundation for the subsequent chapters, laying the groundwork for a deeper understanding of Quadcopters and their role in modern society.

Chapter 2

Modeling of the Quadcopter

This chapter focuses on the dynamic modeling of the Quadcopter system. It begins by providing a detailed description of the system, including its overall structure and flight principles. The chapter then emphasizes the specific state model chosen for this system, highlighting its significance in accurately representing the Quadcopter's dynamics. By thoroughly examining the dynamic modeling aspects, this chapter lays the groundwork for understanding the subsequent control and stability analysis discussed in the following chapters.

2.1 Introduction

To develop a flight controller for a Quadcopter, it is crucial to have a thorough understanding of the aircraft's movements, dynamics, and the corresponding dynamic equations. This knowledge is not only essential for controller design but also ensures that simulations accurately represent the vehicle's behavior when commands are applied.

The Quadcopter falls into the category of highly complex flying systems due to the multitude of physical effects that influence its dynamics, including aerodynamic effects, gravity, gyroscopic effects, friction, and moment of inertia. This complexity arises from the fact that these effects manifest differently in each flight mode. Consequently, the dynamic models proposed for the Quadcopter vary depending on the specific tasks and predefined navigation environments set by the operator.

2.2 General description of the Quadcopter

A Quadcopter is a mobile aerial robot equipped with four rotors, providing it with six degrees of freedom (DOF) in space. Typically, these rotors are positioned at the ends of a cross-shaped frame, while the central area houses the control electronics. To prevent unwanted rotation around the yaw axis, two propellers rotate in one direction, while the other two rotate in the

opposite direction. To enable maneuverability, each pair of propellers spinning in the same direction is positioned at opposite ends of one of the cross's arms.

The operation of a Quadcopter is unique. By intelligently adjusting the motor power, it can ascend/descend, tilt left/right (roll), move forward/backward (pitch), and rotate around its own axis (yaw) [37]. With six degrees of freedom encompassing three rotational and three translational movements, the Quadcopter's control must be achieved using only four actuators. As a result, it is considered an under-actuated system, where the number of inputs is lower than the number of outputs. In the following chapter, we will delve into the dynamic modeling of this system [10] [12]. [13]

2.2.1 Quadcopter movements

In conventional helicopters, the main rotor generates a reactive torque that must be counteracted to prevent the helicopter body from rotating in the opposite direction. This is typically achieved with a tail rotor, but it does not contribute to thrust. In contrast, a Quadcopter addresses this issue by having two rotors spin clockwise and the other two spin counterclockwise, effectively canceling out the reactive torque and enabling stable hovering. Unlike conventional helicopters, all the energy used to counteract rotational movement contributes to thrust.

The Quadcopter achieves basic movements by adjusting the speed of each rotor, altering the generated thrust. Tilting the Quadcopter towards a slower rotor allows for translation along that axis. As a result, the Quadcopter's movements are coupled, meaning that a change in rotor speed affects multiple degrees of freedom. For example, increasing the speed of the port rotor leads to rolling motion, yaw motion, and translation. This coupling allows for control over all six degrees of freedom using only four controls corresponding to the motor torque on each rotor.

The main movements of a Quadcopter include **vertical movement**, **rolling motion**, **pitch motion**, **yaw motion**, and **horizontal translations**.

2.2.1.1 Roll motion

The figure shows how a rolling motion is obtained. In this case, we apply a torque around the x-axis, i.e. by applying a difference in thrust between the rotor 2 and the rotor 4. This movement (rotation around the x axis) is coupled with a movement of translation along the y-axis. [10] [16]

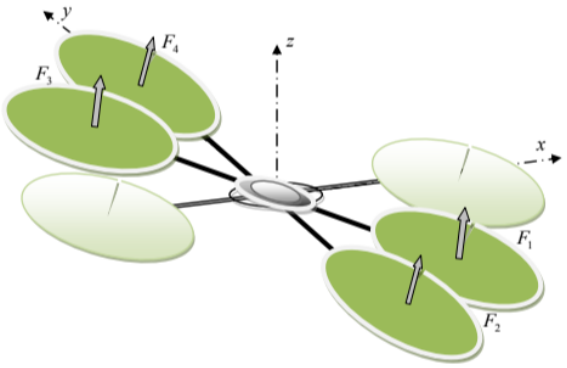

Figure 2.1: Roll motion

2.2.1.2 Pitch motion

The figure shows how a pitch motion is achieved. In this case, we applies a torque around the y-axis, i.e. by applying a difference in thrust between the rotor 1 and rotor 3. This movement (rotation around y) is coupled with a movement of translation along the x axis.

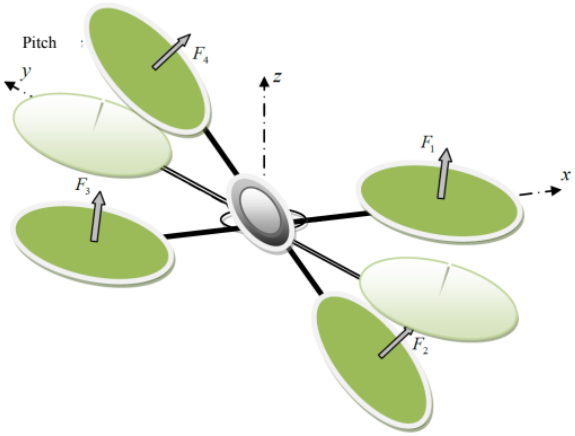

Figure 2.2: Pitch motion

2.2.1.3 Yaw motion

The diagram illustrates the mechanism for achieving yaw motion. In this scenario, a torque is desired around the z-axis, and this is accomplished by creating a speed difference between the rotors 1,3 and 2,4. Unlike other movements, yaw motion is not directly caused by the thrust generated by the rotors but by the reactive torques resulting from their rotation. During this motion, the direction of the resultant thrust force remains unchanged, but the increase in lift force from one pair of rotors must be offset by a corresponding decrease in the other pair to maintain overall thrust equilibrium.

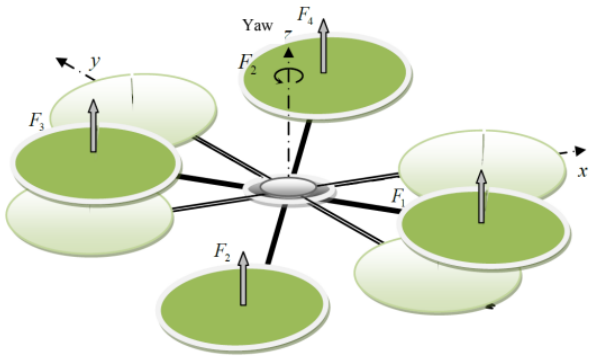

Figure 2.3: Yaw motion

2.2.1.4 Translation movements

The figure below illustrates the method for achieving horizontal translation. When a force along the x or y-axis is desired, the body of the Quadcopter is tilted through pitching or rolling motions. Additionally, all the thrust produced by the rotors is increased to ensure that the vertical component of the thrust remains equal to the force of gravity. By adjusting the tilt and increasing the overall thrust, the Quadcopter is able to generate a net force along the desired horizontal direction for translation.

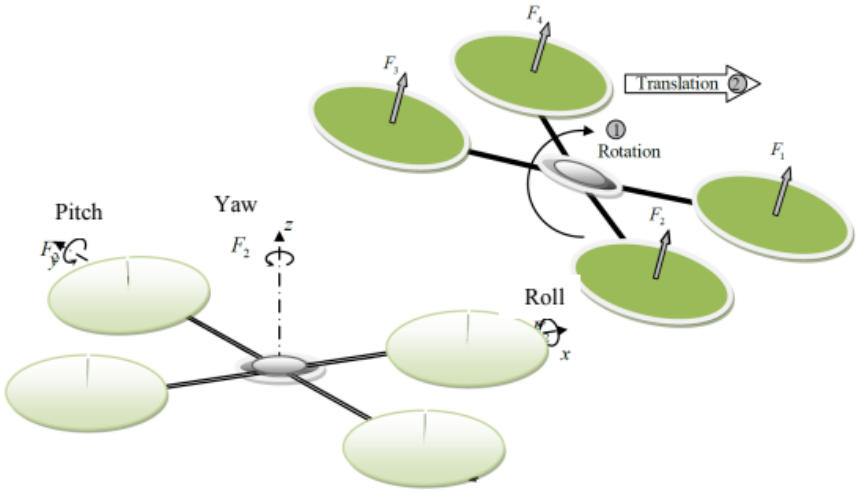

Figure 2.4: Translation movements

2.3 Quadcopter dynamic model

Modeling flying robots is a challenging undertaking due to the highly nonlinear and interconnected dynamics of the system. To provide a clearer understanding of the subsequent dynamic model, the following working hypotheses are considered [16] [18] :

1. The structure of the Quadcopter is supposed to be rigid and symmetrical, which induces that the matrix of inertia will be assumed to be diagonal,
2. The propellers are assumed to be rigid in order to be able to neglect the effect of their deformation during of rotation.
3. The center of mass and the origin of the frame linked to the structure coincide.
4. The lift and drag forces are proportional to the squares of the speed of rotation of the rotors, which is a very close approximation of the behavior aerodynamic.

To evaluate the mathematical model of the Quadcopter we consider a body fixed frame and earth fixed frame. The transformation between the mobile frame and the fixed frame is given by a matrix called the transformation matrix T, which includes the orientation and position of the mobile frame relative to the fixed frame.

We adopt the following axis convention:

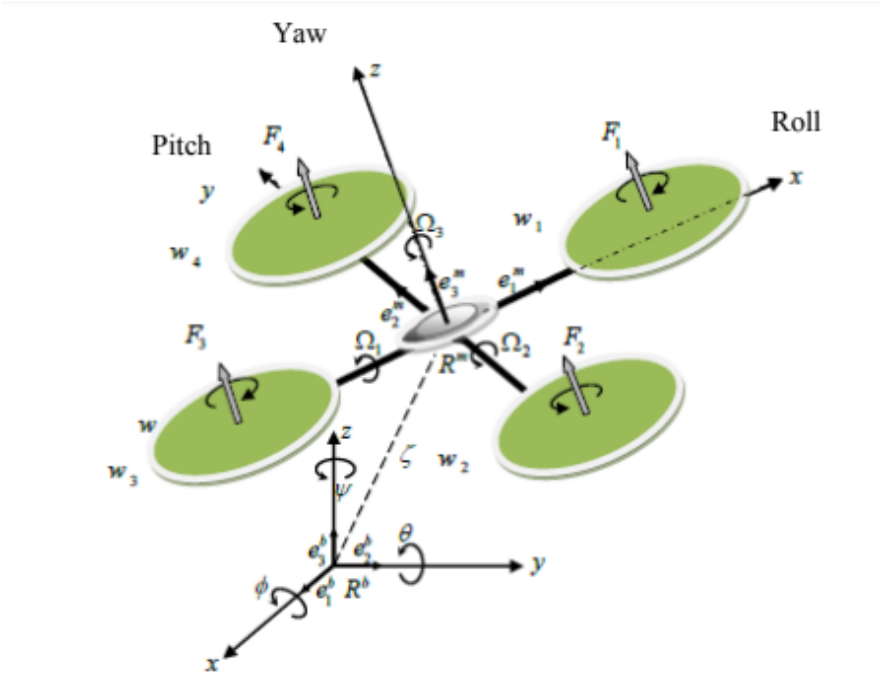

Figure 2.5: The Quadcopter main movements

where

$$T = \begin{bmatrix} R & \zeta \\ 0 & 1 \end{bmatrix} \tag{2.1}$$

with R the rotation matrix (describes the orientation of the moving object), $\zeta = \begin{bmatrix} x & y & z \end{bmatrix}^{\mathrm{T}}$,is the position vector. To determine the elements of the rotation matrix R, we use the Euler angles. [10]

2.3.1 Euler angles

At the beginning, the mobile frame coincides with the fixed frame. Then, the mobile frame undergoes a rotation around the x-axis with a roll angle ($-\pi/2 < \varphi < \pi/2$), followed by a rotation around the y-axis with a pitch angle ($-\pi/2 < \theta < \pi/2$), and finally a rotation around the z-axis with a yaw angle ($-\pi < \psi < \pi$). Therefore, we have the rotation matrix formula R: [16] [17].

$$R = \mathrm{Rot}_z(\psi) \times \mathrm{Rot}_y(\theta) \times \mathrm{Rot}_x(\phi) = \begin{bmatrix} c\psi & -s\psi & 0 \\ s\psi & c\psi & 0 \\ 0 & 0 & 1 \end{bmatrix} \times \begin{bmatrix} c\theta & 0 & s\theta \\ 0 & 1 & 0 \\ -s\theta & 0 & c\theta \end{bmatrix} \times \begin{bmatrix} 1 & 0 & 0 \\ 0 & c\phi & -s\phi \\ 0 & s\phi & c\phi \end{bmatrix} \tag{2.2}$$

$$R = \begin{bmatrix} c\psi c\theta & s\phi s\theta c\psi - s\psi c\phi & c\phi s\theta c\psi + s\psi s\phi \\ s\psi c\theta & s\phi s\theta s\psi + c\psi c\theta & c\phi s\theta s\psi - s\phi c\psi \\ -s\theta & s\phi c\theta & c\phi c\theta \end{bmatrix} \tag{2.3}$$

with : $c = \cos$, et $s = \sin$

2.3.2 Angular velocities

The rotation speeds $\Omega_1, \Omega_2, \Omega_3$ in the fixed frame are expressed as a function of the rotation speeds $\dot{\phi}, \dot{\theta}, \dot{\psi}$ in the moving frame, we have:

$$\Omega = \begin{bmatrix} \Omega_1 \\ \Omega_2 \\ \Omega_3 \end{bmatrix} = \begin{bmatrix} \dot{\phi} \\ 0 \\ 0 \end{bmatrix} + \mathrm{Rot}_x(\phi)^{-1} \begin{bmatrix} 0 \\ \dot{\theta} \\ 0 \end{bmatrix} + \left(\mathrm{Rot}_y(\theta)\,\mathrm{Rot}_x(\phi)\right)^{-1} \begin{bmatrix} 0 \\ 0 \\ \dot{\psi} \end{bmatrix} \tag{2.4}$$

Indeed, the rotation in roll takes place when the marks are still confused. Then, in what concerns the pitch, the vector representing the rotation must be expressed in the fixed frame: it is so multiplied by $\mathrm{Rot}_x(\phi)^{-1}$. Similarly, the vector representing the yaw rotation must be expressed in the fixed frame which has already undergone two rotations. We thus arrive at:

$$\Omega = \begin{bmatrix} \Omega_x \\ \Omega_y \\ \Omega_z \end{bmatrix} = \begin{bmatrix} \dot{\phi} \\ 0 \\ 0 \end{bmatrix} + \begin{bmatrix} 0 \\ \dot{\theta}c\phi \\ -\dot{\theta}s\phi \end{bmatrix} + \begin{bmatrix} -\dot{\psi}s\theta \\ \dot{\psi}s\phi c\theta \\ \dot{\psi}c\phi c\theta \end{bmatrix} = \begin{bmatrix} \dot{\phi} - \dot{\psi}s\theta \\ \dot{\theta}c\phi + \dot{\psi}s\phi c\theta \\ \dot{\psi}c\phi c\theta - \dot{\theta}s\phi \end{bmatrix} \tag{2.5}$$

$$\Omega = \begin{bmatrix} 1 & 0 & -s\theta \\ 0 & c\phi & s\phi c\theta \\ 0 & -s\phi & c\phi c\theta \end{bmatrix} \times \begin{bmatrix} \dot{\phi} \\ \dot{\theta} \\ \dot{\psi} \end{bmatrix} \tag{2.6}$$

When the Quadcopter makes small rotations, the following approximations can be made:

$$c\phi = c\theta = c\psi = 1, \text{ et } s\phi = s\theta = s\psi = 0. \tag{2.7}$$

so the angular velocity will be:

$$\Omega = \begin{bmatrix} \dot{\phi} & \dot{\theta} & \dot{\psi} \end{bmatrix}^T \tag{2.8}$$

2.3.3 Linear speeds

Linear speeds v_x^b, v_y^b, v_z^b in the fixed frame according to the linear velocities v_x^m, v_y^m, v_z^m in the moving frame are given by:

$$v = \begin{bmatrix} v_x^b \\ v_y^b \\ v_z^b \end{bmatrix} = R \times \begin{bmatrix} v_x^m \\ v_y^m \\ v_z^m \end{bmatrix} \tag{2.9}$$

2.3.4 Physical effects acting on the Quadcopter

2.3.4.1 Forces:

The forces acting on the system are:

The weight of the Quadcopter: it is given by $P = mg$, where: m is the total mass and g the gravity.

The thrust forces: which are forces caused by the rotation of the motors, they are perpendicular to the plane of the propellers. These forces are proportional to the square of the speed engine rotation:

$$F_i = b\omega_i^2 \tag{2.10}$$

with: $i = \overline{1:4}$, And b is the lift coefficient, it depends on the shape and number of the blades and the air density.

Drag forces: The drag force is the coupling between a pressure force and the force viscous friction, in this case there are two drag forces acting on the system that they are:

- The drag in the propellers: it acts on the blades, it is proportional to the density of the air, the shape of the blades and the square of the speed of rotation of the propeller, it is given by the following equation:

$$T_b = d\omega^2 \tag{2.11}$$

with d is the drag coefficient it depends on the manufacture of the propeller.

- The drag along the (x, y, z) axes: it is caused by the motion of the Quadcopter's body.

$$F_t = K_{ft} v \tag{2.12}$$

with : K_{ft} the translational drag coefficient and V linear speed.

2.3.4.2 The moments

There are several moments acting on the Quadcopter, these moments are due to the forces of thrust and drag and gyroscopic effects.

Moments due to thrust forces:

- The rotation around the x axis: it is due to the moment created by the difference between the forces of lift of rotors 2 and 4, this moment is given by the following equation:

$$M_x = l\left(F_4 - F_2\right) = lb\left(\omega_4^2 - \omega_2^2\right) \tag{2.13}$$

where l is the length of the arm between the rotor and the center of gravity of the Quadcopter.

- The rotation around the y axis: it is due to the moment created by the difference between the forces lift of rotors 1 and 3, this moment is given by the following equation:

$$M_y = l\left(F_3 - F_1\right) = lb\left(\omega_3^2 - \omega_1^2\right) \tag{2.14}$$

Moments due to drag forces:

- The rotation around the z axis: it is due to a reactive torque caused by the torques of drag in each propeller, this moment is given by the following equation:

$$M_z = d\left(\omega_1^2 - \omega_2^2 + \omega_3^2 - \omega_4^2\right) \tag{2.15}$$

- Moment resulting from aerodynamic friction, it is given by:

$$M_a = K_{fa}\Omega^2 \tag{2.16}$$

with, K_{fa} :: The coefficient of aerodynamic friction and Ω is the angular velocity.

2.3.4.3 Gyroscopic effect

The gyroscopic effect is defined as the difficulty in changing the position or orientation of the plane of rotation of a rotating mass. The term "gyroscopic effect" is named in reference to the operation of a gyroscope, a motion control device used in aviation (from the Greek words gyro meaning rotation and scope meaning observer).

In our case, there are two gyroscopic moments: the first is the gyroscopic moment of the propellers, and the other is the gyroscopic moment due to the movements of the Quadcopter.

- Gyroscopic moment of the propellers: it is given by the following equation:

$$M_{gh} = \sum_{1}^{4} \Omega \wedge J_r[00\ (-1)^{i+1}\omega_i]^T \tag{2.17}$$

  with J_r is the inertia of the rotors.

- Gyroscopic moment due to the movements of the Quadcopter: it is given by the equation :

$$M_{gm} = \Omega \wedge J\Omega \tag{2.18}$$

  where J is the inertia of the system.

2.3.5 Development of the Mathematical Model according to Newton-Euler

Using the Newton-Euler formulation, the equations are written as [13]:

$$\begin{cases} \dot{\zeta} = v \\ m\ddot{\zeta} = F_f + F_t + F_g \\ \dot{R} = RS(\Omega) \\ J\dot{\Omega} = -\Omega \wedge J\Omega + M_f - M_a - M_{gh} \end{cases} \tag{2.19}$$

where: $\dot{\zeta}$ is the position vector of the Quadcopter; m is the total mass of the Quadcopter; Ω is the angular velocity expressed in the fixed frame; R is the rotation matrix; $\wedge$ represents the cross product, and J is a symmetric inertia matrix of dimension (3×3), it is given by

$$J = \begin{bmatrix} I_x & 0 & 0 \\ 0 & I_y & 0 \\ 0 & 0 & I_z \end{bmatrix} \tag{2.20}$$

$S(\Omega)$: is the antisymmetric matrix; for a velocity vector

$$\Omega = \begin{bmatrix} \Omega_1 & \Omega_2 & \Omega_3 \end{bmatrix}^T \tag{2.21}$$

it is given by:

$$S(\Omega) = \begin{bmatrix} 0 & -\Omega_3 & \Omega_2 \\ \Omega_3 & 0 & -\Omega_1 \\ -\Omega_2 & \Omega_1 & 0 \end{bmatrix} \tag{2.22}$$

F_f: is the total force generated by the four rotors, it is given by:

$$F_f = R \times \begin{bmatrix} 0 & 0 & \sum_{i=1}^{4} F_i \end{bmatrix}^T F_i = b\omega_i^2 \tag{2.23}$$

F_t: the drag force along the axes (x, y, z), it is given by:

$$F_t = \begin{bmatrix} -K_{ftx} & 0 & 0 \\ 0 & -K_{fty} & 0 \\ 0 & 0 & -K_{ftz} \end{bmatrix} \dot{\zeta} \tag{2.24}$$

$K_{ftx}, K_{fty}, K_{ftz}$ stand for drag coefficients, F_g represents force of gravity, it is given by:

$$F_g = \begin{bmatrix} 0 \\ 0 \\ -mg \end{bmatrix} \tag{2.25}$$

M_f: moment caused by thrust and drag forces.

$$M_f = \begin{bmatrix} l\,(F_4 - F_2) \\ l\,(F_3 - F_1) \\ d\,(\omega_1^2 - \omega_2^2 + \omega_3^2 - \omega_4^2) \end{bmatrix} \tag{2.26}$$

M_a : moment resulting from aerodynamic friction, it is given by:

$$M_a = \begin{bmatrix} K_{fax}\dot{\phi}^2 \\ K_{fay}\dot{\theta}^2 \\ K_{faz}\dot{\psi}^2 \end{bmatrix} \tag{2.27}$$

$K_{fax}, K_{fay}, K_{fac}$: The aerodynamic friction coefficients [16].

2.3.5.1 Translational motion equations

We have :

$$m\ddot{\zeta} = F_f + F_t + F_g \tag{2.28}$$

We replace each force by its formula, we find:

$$m\begin{bmatrix}\ddot{x}\\ \ddot{y}\\ \ddot{z}\end{bmatrix}=\begin{bmatrix}c\phi c\psi s\theta+s\phi s\psi\\ c\phi s\theta s\psi-s\phi c\psi\\ c\phi c\theta\end{bmatrix}\sum_{i=1}^{4}F_i-\begin{bmatrix}K_{ftx}\dot{x}\\ K_{fty}\dot{y}\\ K_{ftz}\dot{z}\end{bmatrix}-\begin{bmatrix}0\\ 0\\ mg\end{bmatrix} \tag{2.29}$$

We then obtain the differential equations which define the translational movement:

$$\begin{cases}\ddot{x}=\frac{1}{m}(c\phi c\psi s\theta+s\phi s\psi)\left(\sum_{i=1}^{4}F_i\right)-\frac{K_{ftx}}{m}\dot{x}\\ \ddot{y}=\frac{1}{m}(c\phi s\theta s\psi-s\phi c\psi)\left(\sum_{i=1}^{4}F_i\right)-\frac{K_{fyy}}{m}\dot{y}\\ \ddot{z}=\frac{1}{m}(c\phi c\theta)\left(\sum_{i=1}^{4}F_i\right)-\frac{K_{ftz}}{m}\dot{z}-g\end{cases} \tag{2.30}$$

2.3.5.2 Rotational Motion Equations

we have :

$$J\dot{\Omega}=-M_{gh}-M_{gh}-M_a+M_f \tag{2.31}$$

We substitute each moment by the corresponding formula, one abtains:

$$\begin{aligned}\begin{bmatrix}I_x&0&0\\0&I_y&0\\0&0&I_z\end{bmatrix}\begin{bmatrix}\ddot{\phi}\\ \ddot{\theta}\\ \ddot{\psi}\end{bmatrix}=&-\begin{bmatrix}\dot{\phi}\\ \dot{\theta}\\ \dot{\psi}\end{bmatrix}\wedge\left(\begin{bmatrix}I_x&0&0\\0&I_y&0\\0&0&I_z\end{bmatrix}\begin{bmatrix}\dot{\phi}\\ \dot{\theta}\\ \dot{\psi}\end{bmatrix}\right)-\begin{bmatrix}J_r\bar{\Omega}_r\dot{\theta}\\ -J_r\bar{\Omega}_r\dot{\phi}\\ 0\end{bmatrix}\\ &-\begin{bmatrix}K_{fax}\dot{\phi}^2\\ K_{fay}\dot{\theta}^2\\ K_{faz}\dot{\psi}^2\end{bmatrix}+\begin{bmatrix}lb\left(\omega_4^2-\omega_2^2\right)\\ lb\left(\omega_3^2-\omega_1^2\right)\\ d\left(\omega_1^2-\omega_2^2+\omega_3^2-\omega_4^2\right)\end{bmatrix}\end{aligned} \tag{2.32}$$

We then obtain the differential equations defining the rotational movement:

$$\begin{cases}I_x\ddot{\phi}=-\dot{\theta}\dot{\psi}\left(I_z-I_y\right)-J_r\bar{\Omega}_r\dot{\theta}-K_{fax}\dot{\phi}^2+lb\left(\omega_4^2-\omega_2^2\right)\\ I_y\ddot{\theta}=\dot{\phi}\dot{\psi}\left(I_z-I_x\right)+J_r\bar{\Omega}_r\dot{\phi}-K_{fay}\dot{\theta}^2+lb\left(\omega_3^2-\omega_1^2\right)\\ I_z\ddot{\psi}=-\dot{\phi}\dot{\theta}\left(I_y-I_x\right)-K_{faz}\dot{\psi}^2+d\left(\omega_1^2-\omega_2^2+\omega_3^2-\omega_4^2\right)\end{cases} \tag{2.33}$$

with :

$$\bar{\Omega}_{rr}=\omega_1-\omega_2+\omega_3-\omega_4 \tag{2.34}$$

Accordingly, the full dynamic model that governs the Quadcopter is as follows:

$$\begin{cases} \ddot{\phi} = \frac{(I_y - I_z)}{I_x}\dot{\theta}\dot{\psi} - \frac{J_r}{I_x}\bar{\Omega}_r\dot{\theta} - \frac{K_{fax}}{I_x}\dot{\phi}^2 + \frac{l}{I_x}u_2 \\ \ddot{\theta} = \frac{(I_z - I_x)}{I_y}\dot{\phi}\dot{\psi} + \frac{J_r}{I_y}\bar{\Omega}_r\dot{\phi} - \frac{K_{far}}{I_y}\dot{\theta}^2 + \frac{l}{I_y}u_3 \\ \ddot{\psi} = \frac{(I_x - I_y)}{I_z}\dot{\theta}\dot{\phi} - \frac{K_{fc}}{I_z}\dot{\psi}^2 + \frac{1}{I_z}u_4 \\ \ddot{x} = -\frac{K_{fxx}}{m}\dot{x} + \frac{1}{m}u_x u_1 \\ \ddot{y} = -\frac{K_{fyy}}{m}\dot{y} + \frac{1}{m}u_y u_1 \\ \ddot{z} = -\frac{K_{fzz}}{m}\dot{z} - g + \frac{\cos(\phi)\cos(\theta)}{m}u_1 \end{cases} \tag{2.35}$$

with :

$$\begin{cases} u_x = (c\phi c\psi s\theta + s\phi s\psi) \\ u_y = (c\phi s\theta s\psi - s\phi c\psi) \end{cases} \tag{2.36}$$

and :

$$\begin{bmatrix} u_1 \\ u_2 \\ u_3 \\ u_4 \end{bmatrix} = \begin{bmatrix} b & b & b & b \\ 0 & -lb & 0 & lb \\ -lb & 0 & lb & 0 \\ d & -d & d & -d \end{bmatrix} \begin{bmatrix} \omega_1^2 \\ \omega_2^2 \\ \omega_3^2 \\ \omega_4^2 \end{bmatrix} \tag{2.37}$$

from (2.36), one gets the following

$$\begin{cases} \phi_d = \arcsin\left(u_x \sin\left(\psi_d\right) - u_y \cos\left(\psi_d\right)\right) \\ \theta_d = \arcsin\left(\frac{(u_x \cos(\psi_d) + u_y \sin(\psi_d))}{\cos(\phi_d)}\right) \end{cases} \tag{2.38}$$

In our study we consider the following dynamic model because it is specifically suited for the study of rotational motion.

$$\begin{cases} \ddot{\phi} = \frac{(I_y - I_z)}{I_x}\dot{\theta}\dot{\psi} - \frac{J_r}{I_x}\bar{\Omega}_r\dot{\theta} - \frac{K_{fax}}{I_x}\dot{\phi}^2 + \frac{l}{I_x}u_2 \\ \ddot{\theta} = \frac{(I_z - I_x)}{I_y}\dot{\phi}\dot{\psi} + \frac{J_r}{I_y}\bar{\Omega}_r\dot{\phi} - \frac{K_{fay}}{I_y}\dot{\theta}^2 + \frac{l}{I_y}u_3 \\ \ddot{\psi} = \frac{(I_x - I_y)}{I_z}\dot{\theta}\dot{\phi} - \frac{K_{faz}}{I_z}\dot{\psi}^2 + \frac{1}{I_z}u_4 \end{cases} \tag{2.39}$$

Given our emphasis on Quadcopter control in the presence of external disturbances that may impact its stability, it becomes necessary to modify the nonlinear model (2.39). This can be achieved by incorporating the external disturbances into the model. Furthermore, Let $\omega_\theta = \dot{\theta}, \omega_\phi = \dot{\phi}, \omega_\psi = \dot{\psi}$; thus, one can write:

$$\begin{cases} \dot{\omega}_\phi = \frac{(I_y - I_z)}{I_x}\omega_\theta\omega_\psi - \frac{J_r}{I_x}\bar{\Omega}_r\omega_\theta - \frac{K_{fax}}{I_x}\omega_\phi^2 + \frac{l}{I_x}u_2 + d_\phi \\ \dot{\omega}_\theta = \frac{(I_z - I_x)}{I_y}\omega_\phi\omega_\psi + \frac{J_r}{I_y}\bar{\Omega}_r\omega_\phi - \frac{K_{fay}}{I_y}\omega_\theta^2 + \frac{l}{I_y}u_3 + d_\theta \\ \dot{\omega}_\psi = \frac{(I_x - I_y)}{I_z}\omega_\theta\omega_\phi - \frac{K_{faz}}{I_z}\omega_\psi^2 + \frac{1}{I_z}u_4 + d_\psi \end{cases} \tag{2.40}$$

2.3.6 Rotor dynamics

Generally the motors used in Quadcopters are DC motors. The dynamics of the rotor is approximated to that of a DC motor, it is given by the following differential equations:

$$J_r\dot{\omega}_i = \tau_i - Q_i \quad , i \in \{1, 2, 3, 4\} \tag{2.41}$$

with: τ_i is the input torque, and $Q_i = d\omega_i^2$ is the resistive torque generated by rotor i.

To achieve the objectives of Quadcopter control, a velocity control loop is often required. Firstly, we need to determine the desired velocities $\omega_{d,i}$ corresponding to the control input values provided by the controller. These velocities can be calculated as follows:

$$\varpi_d = M^{-1}U \tag{2.42}$$

with : $\varpi_d = (\omega_{d1}^2, \omega_{d2}^2, \omega_{d3}^2, \omega_{d4}^2)^T, U = (u_1, u_2, u_3, u_4)^T$ and M is a non-singular matrix, it is obtained from (2.37).

The objective is to synthesize a controller so that $\omega_i \to \omega_{d,i}$ when $t \to \infty$ using torques τ_i.

We define the speed error:

$$\tilde{\omega}_i = \omega_i - \omega_{d,i} \tag{2.43}$$

A control law is developed in [16] [17], it is given by:

$$\tau_i = Q_i + J_r\dot{\omega}_{d,i} - k_i\tilde{\omega}_i \tag{2.44}$$

with $k_i, i \in \{1, 2, 3, 4\}$ are positive gains.

By substituting the control law into (2.41), we obtain:

$$\dot{\tilde{\omega}}_i = -\frac{k_i}{J_r}\tilde{\omega}_i \tag{2.45}$$

This equation represents the error dynamics and illustrates the exponential convergence of ω_i towards $\omega_{d,i}$ as t approaches infinity. This convergence signifies the stability of the Quadcopter by ensuring that its controls approach the desired values.

In practice, the Quadcopter is controlled by manipulating the power supply voltages applied to its four motors. To command these motors effectively, we need to determine the input voltage for each motor. Assuming negligible motor inductance and the use of identical motors, we can calculate the input voltage for each motor in the following manner:

$$v_i = \frac{R_a}{k_m k_g}\tau_i + k_m k_g \omega_i \tag{2.46}$$

with R_a is the resistance of the motor, k_m is the motor torque constant, k_g is the gain of the reducer.

2.4 Simulation of Quadcopter open-loop model

The Quadcopter nonlinear model is simulated in using Matlab software. The parameter of the system are shown in the table below:

Table 2.1: Parameters of the Quadcopter

Parameter	Value	Parameter	Value
m	$0,486$ kg	K_{fay}	$5,5670 \times 10^{-4}$ N/rad/s
g	$9,806$ m/s^2	K_{faz}	$6,3540 \times 10^{-4}$ N/rad/s
l	$0,25$ m	K_{ftx}	$5,5670 \times 10^{-4}$ N/m/s
b	$2,9842 \times 10^{-5}$ N/rad/s	K_{fty}	$5,5670 \times 10^{-4}$ N/m/s
d	$3,2320 \times 10^{-7}$ N.m/rad/s	K_{ftz}	$6,3540 \times 10^{-4}$ N/m/s
J_r	$2,8385 \times 10^{-5}$ kg.m^2	k_i	$20 \times J_r$
I_x	$3,8278 \times 10^{-3}$ kg.m^2	k_m	$4,3 \times 10^{-3}$ N.m/A
I_y	$3,8288 \times 10^{-3}$ kg.m^2	k_g	5,6
I_z	$7,6566 \times 10^{-3}$ kg.m^2	R_a	$0,67\Omega$
K_{fax}	$5,5670 \times 10^{-4}$ N/rad/s	v_n	12v

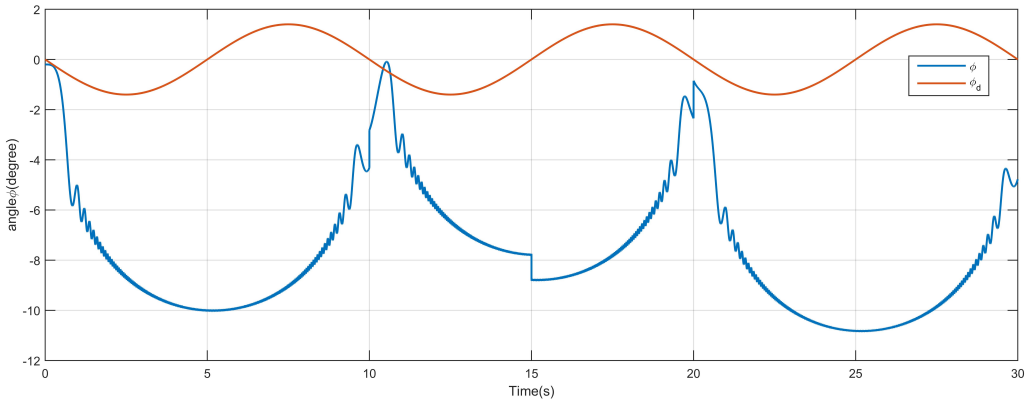

Figure 2.6: Evolution of the roll angle.

The plot clearly demonstrates that the angle ϕ exhibits oscillatory behavior starting from the initial instant (0s) onward. This oscillation introduces instability to the angle with respect to the desired value ϕ_d.

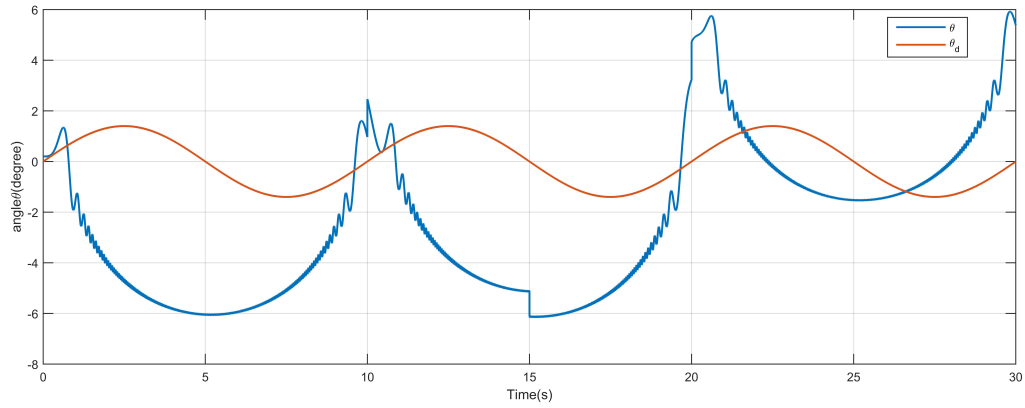

Figure 2.7: Evolution of the pitch angle.

The angular curve θ, starting from the initiation of the experiment, exhibits instability with respect to θ_d (desired angle).

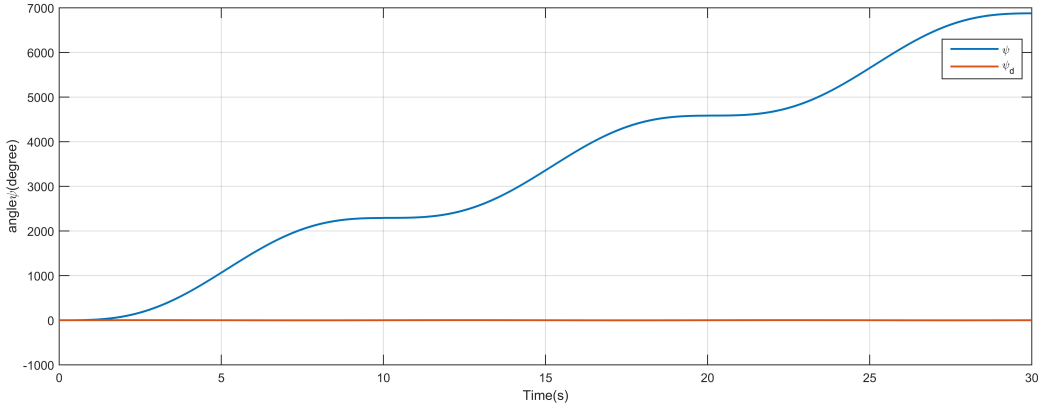

Figure 2.8: Evolution of the yaw angle.

The graph clearly illustrates that the angle ψ experiences diverging oscillations throughout the given time period, starting from the initial moment (0s). This oscillatory pattern results in instability of the angle in relation to the desired angle ψ_d.

2.5 Conclusion

This chapter provides the reader with preliminary insights into the fundamental concepts of aerial robotics and their underlying operational principles. The Quadcopter, a prominent aerial robotic platform that has garnered significant research attention in recent years, is the focal point of investigation. This system comprises four rotors, wherein a pair rotates in one direction while the other pair rotates in the opposite direction. By modulating the

rotational velocities of these rotors, the Quadcopter exhibits a versatile range of translational and rotational maneuvers.

The employment of the Newton-Euler formalism has enabled the derivation of the dynamic model for the Quadcopter. Analysis of the resulting model reveals the underactuated nature of the Quadcopter system. Furthermore, the model exhibits notable complexities, nonlinearity, and intricate state interdependencies, which are manifestly evident. In the forthcoming chapter, two control architectures, namely PID and Synergitic controllers, will be introduced as viable approaches to address the control challenges associated with the Quadcopter system.

Chapter 3

Design of controllers

3.1 Introduction

PID control is a very simple and powerful method for controlling a variety of processes, including temperature [19] [18] [1].

Suppose you have a Process (e.g. a temperature chamber with heater and compressor) which produces a measurable Process Variable y (e.g. the temperature measurement in the chamber). The Process is controlled via a drive signal u that comes from the controller, and your goal is to match the PV to a target value, also known as the Setpoint.

The acronym PID stands for "Proportional, Integral, and Derivative". Each cycle, the PID controller calculates the next output value using the measured error between the Setpoint and measured Process Variable, as shown in the above diagram. It computes the output value as the sum of the following three values:

- Proportional term: take the error and multiply it by a constant K_p.
- Integral term: take the cumulative total error and multiply it by a constant K_i.
- Derivative term: take the rate of change in error and multiply it by a constant K_d.

Finally, it adds all three of the above values together to produce the final output u for that cycle where:

- $u(t)$ is the drive coming from the Controller, into the Process, at time t.
- $e(t) = y_d(t) - y(t)$ is the difference between the setpoint and measured process variable at time t.
- K_p, K_i, K_d are the respective P, I, and D constants.

The performance of the PID algorithm depends heavily on whether appropriate PID parameters have been selected. If the PID constants are a good fit for the process, the control will converge smoothly. On the other hand, if the PID constants are chosen poorly, the system may oscillate or destabilize and lose control.

PID constants are ultimately determined by the user and can be refined through a combination of tuning algorithms and trial / error. Two popular methods for PID tuning are the Ziegler-Nichols and Åström-Hägglund tuning methods [1].

3.2 PID controller

3.2.1 A brief review of the PID controller

We now consider each of the terms, assuming that the others are zero. With $Ki = Kd = 0$, we simply have $u(t) = Kpe(t)$. Thus at any instant in time, the control is proportional to the error. It is a function of the present value of the error. The larger the error, the larger the control signal. One way to look at this term is that the farther away from the desired point we are, the harder we try. As we get closer, we don't try quite as hard. If we are right on the target, we stop trying. As can be seen by this analogy, when we are close to the target, the control essentially does nothing. Thus, if the system drifts a bit from the target, the control does almost nothing to bring it back. Thus enters the integral term [8] [9]. Assuming now that $K_p = K_d = 0$ we simply have:

$$u(t) = K_i \int_0^t e(\tau)d\tau \tag{3.1}$$

The addition of this integral makes the open-loop forward path of Type 1. Thus, the system, if stable, is guaranteed to have zero steady-state error to a step input. This can also be viewed as an application of the internal model principle. If $e(t)$ is non-zero for any length of time (for example, positive), the control signal gets larger and large as time goes on. It thus forces the plant to react in the event that the plant output starts to drift. We can think of the integral term as an accumulation of the past values of the error. It is not uncommon for the integral gain to be related to the proportional gain by [20]:

$$K_i = \frac{K_p}{\tau_i} \tag{3.2}$$

where τ_i is the integral time. Generally, by itself, the I term is not used. It is more commonly used with the P term to give a PI control. The I term tends to slow the system reactions down. In order to speed up the system responses, we add the derivative term. Assuming now that $K_p = K_i = 0$ we have [19]

$$u(t) = K_d \frac{de(t)}{dt} \tag{3.3}$$

that is that the control is based on the rate of change of the error. The more quickly the error responds, the larger the control effort. This changing of the error indicates where the error is going. We can thus think of the derivative term as being a function that is that the control is based on the rate of change of the error. The more quickly the error responds, the larger the control effort. This changing of the error indicates where the error is going.

3.2.2 PID controller for the Quadcopter attitude control

The PID controller is applied to the Quadcopter system. The controller scheme for each Euler angle is presented in the subsequent figures.

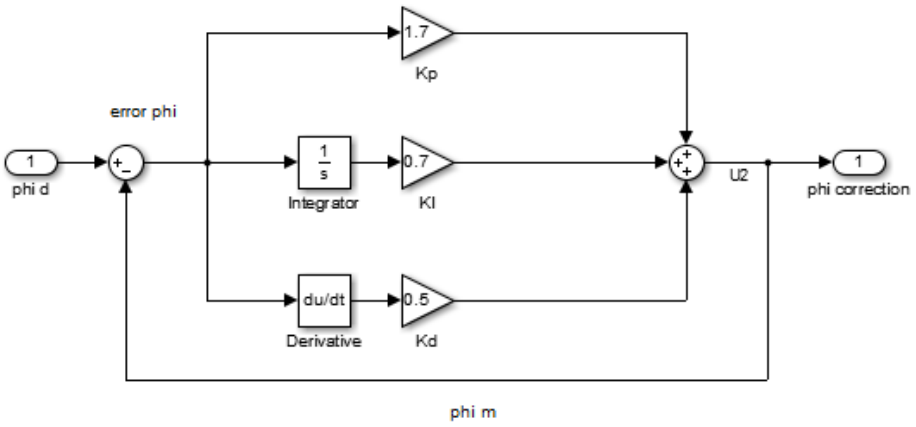

Figure 3.1: Diagram of roll controlling

The control scheme of the rolling motion is shown in figure 3.1 above. The corresponding equation is as follows:

$$u_2(t) = K_p e\phi(t) + K_i \int_0^t e\phi(\tau)d\tau + K_d \frac{d}{dt} e\phi(t) \tag{3.4}$$

where $u_2(t)$ is the control signal that is responsible for the control of the roll angle ϕ.

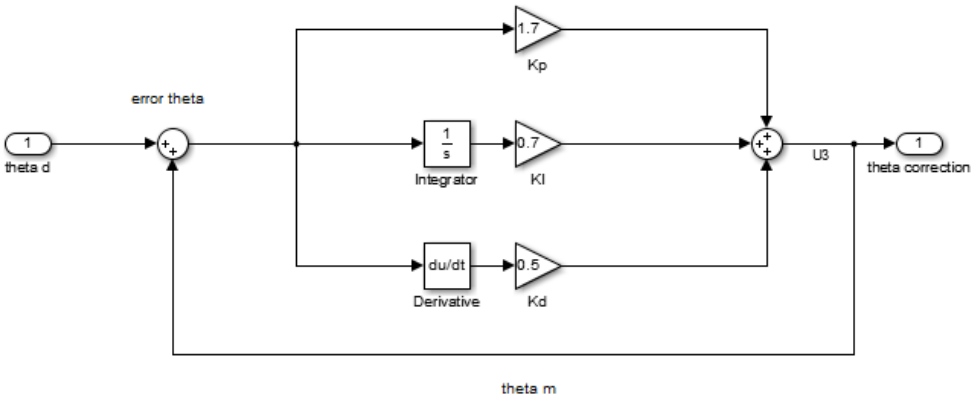

Figure 3.2: Diagram of pitch controlling

The control scheme of the pitching motion is shown in figure 3.2 above. The corresponding equation is as follows:

$$u_3(t) = K_p e\theta(t) + K_i \int_0^t e\theta(\tau)d\tau + K_d \frac{d}{dt} e\theta(t) \tag{3.5}$$

where $u_3(t)$ is the control signal that is responsible for the control of the roll angle θ.

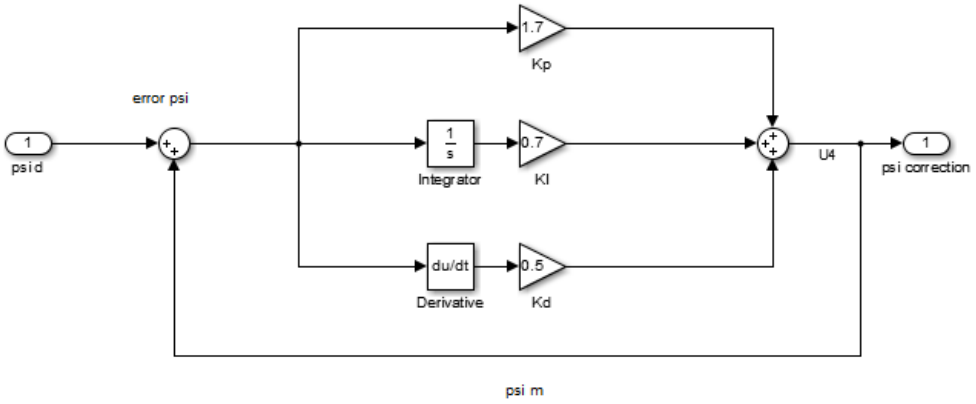

Figure 3.3: Diagram of yaw controlling

The control scheme of the pitching motion is shown in figure 3.3 above. The corresponding equation is as follows:

$$u_4(t) = K_p e\psi(t) + K_i \int_0^t e\psi(\tau)d\tau + K_d \frac{d}{dt} e\psi(t) \tag{3.6}$$

where $u_4(t)$ is the control signal that is responsible for the control of the roll angle ψ.

3.2.3 Simulation of Quadcopter closed-loop model

The Quadcopter attitude control scheme is illustrated in Figure 3.4 below. It consists of three blocks, namely, Bloc A, Block B and block C. Each block of the control scheme will be presented in the subsequent development.

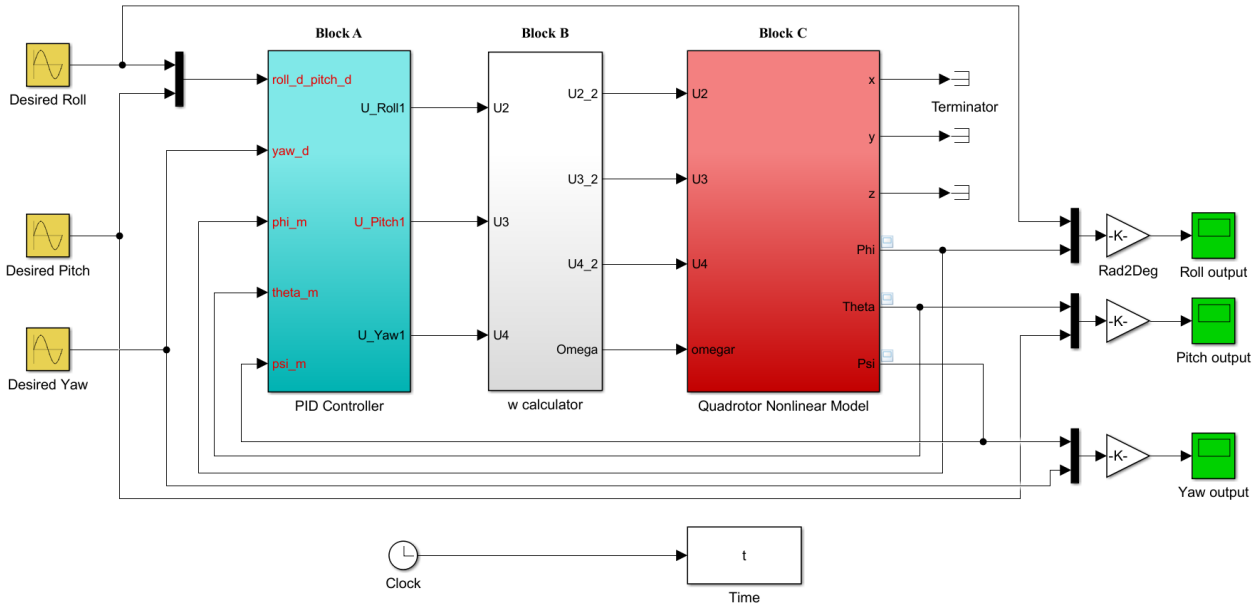

Figure 3.4: Closed-loop scheme

3.2.3.1 Block A: Controller block

The controller block consists of the sub-blocks shown in figure below. It illustrates the decentralised architecture of the PID controller.

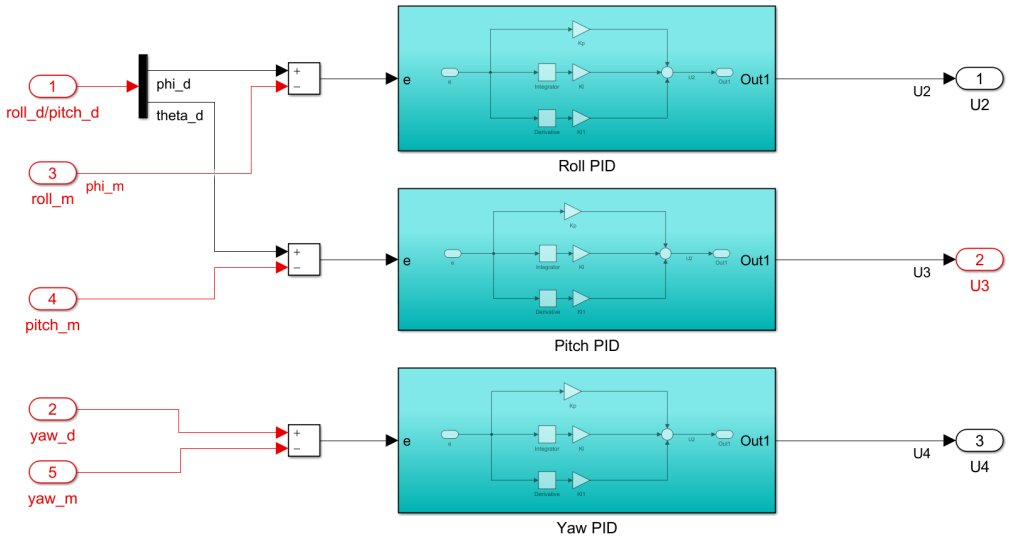

Figure 3.5: Bloc A

3.2.3.2 Block B: ω_i calculator

The ω_i calculator block consists of the sub-blocks shown in figure below. The ω_i are calculated by using equation (2.37).

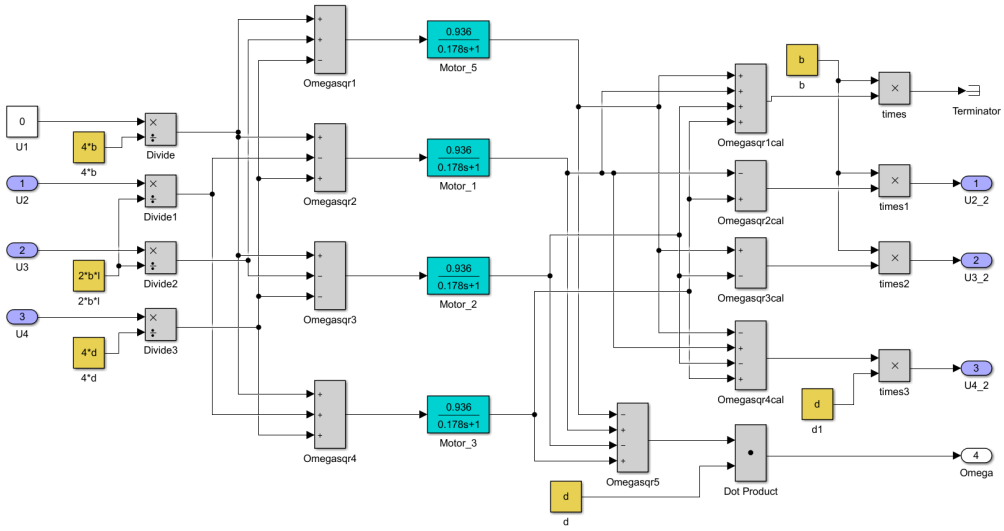

Figure 3.6: Bloc B

3.2.3.3 Block C: Quadcopter Nonlinear Model

That block consists the sub-blocks shown below. They contain the Quadcopter nonlinear model given by equation (2.40).

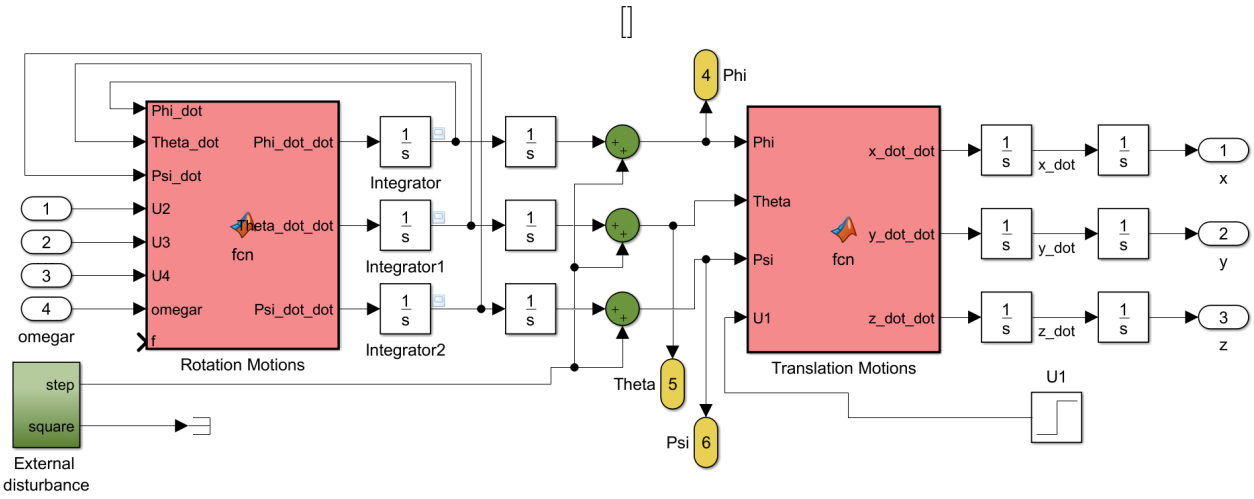

Figure 3.7: Bloc C

3.2.3.4 Simulation results

The obtained simulation results are shown in the figures below. The PID gains used are given in the following table:

Table 3.1: Paramétres du PID

Angles	PID gains		
ϕ	$K_P = 4$	$K_I = 1.5$	$K_D = 3$
θ	$K_P = 4$	$K_I = 1.5$	$K_D = 3$
ψ	$K_P = 2$	$K_I = 0.7$	$K_D = 1.5$

The robustness of the PID controller is rigorously assessed by subjecting it to external disturbances. The applied external disturbances to the Quadcopter system are precisely controlled and measured, with magnitudes of $d_\phi = 1.5, \text{Nm}$, $d_\theta = 1.5, \text{Nm}$, and $d_\psi = 1.5, \text{Nm}$, occurring at well-defined time instances: $t = 10, \text{s}$, $t = 15, \text{s}$, and $t = 20, \text{s}$, respectively. These disturbances are introduced to evaluate the controller's resilience against real-world conditions.

Remarkably, despite the presence of these perturbations, the PID controller consistently exhibits robust performance by effectively stabilizing the Quadcopter system. The achieved stability is evident in Figures 3.8, 3.9 and 3.10, which illustrates the tracking of the Quadcopter's angles towards their desired orientations. Notably, a slightly big deviation is observed at the moments of disturbance occurrence, reflecting the controller's active effort to minimize the discrepancy between the actual angles and their reference values. Consequently, the primary objective of minimizing tracking errors is admirably fulfilled, as shown in figures 3.11-3.13.

Moreover, Figures 3.14-3.16 provides further insights into the controller's effectiveness, showcasing the control signals applied to the Quadcopter during the disturbance periods. Notably,

these control signals remain within an acceptable range, exhibiting desirable characteristics such as low magnitude and smoothness. This is a critical aspect when transitioning from simulated environments to real-world implementations, as it ensures the safe and reliable operation of the Quadcopter under practical conditions.

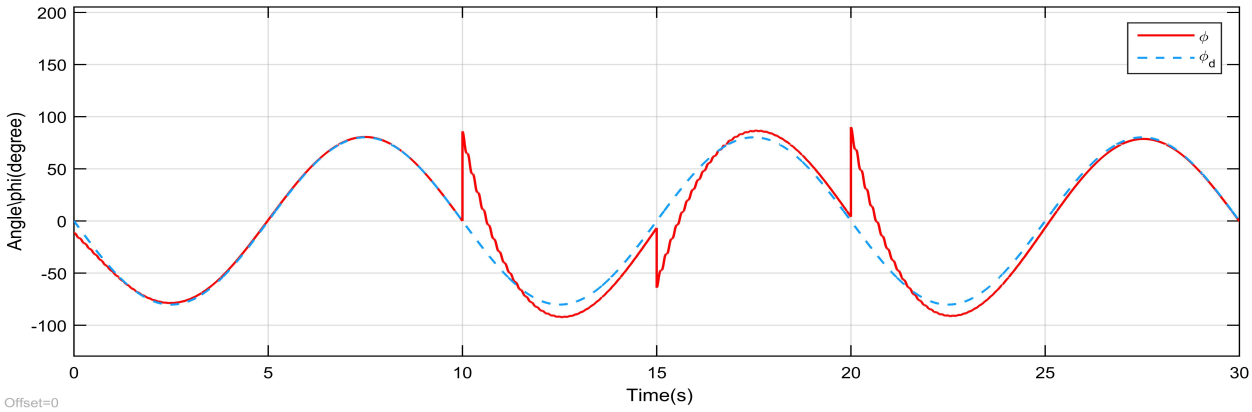

Figure 3.8: Graphic curve of the angle ϕ

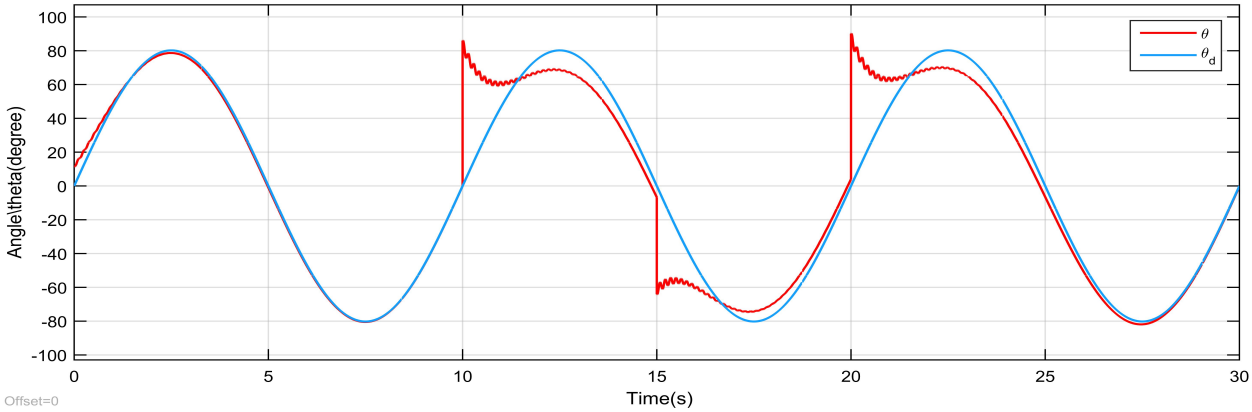

Figure 3.9: graphic curve of the angle θ

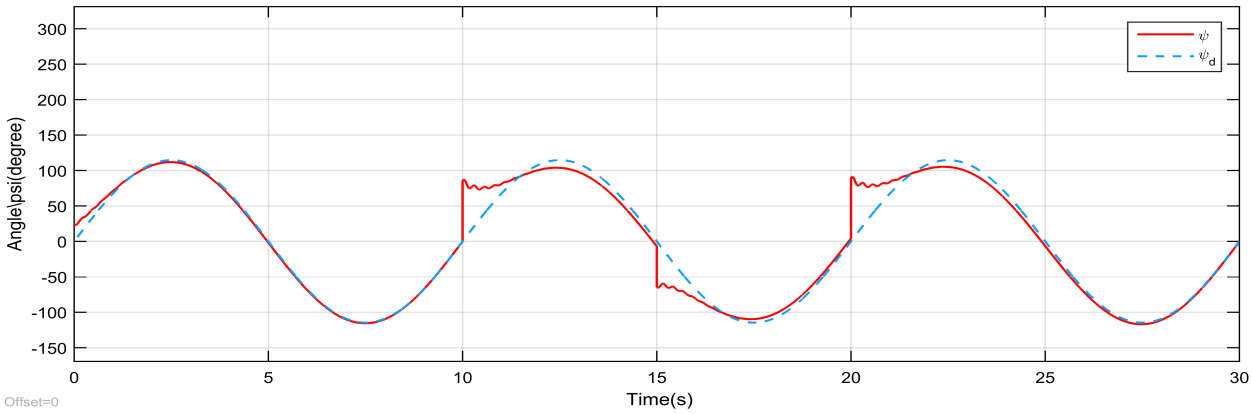

Figure 3.10: graphic curve of the angle ψ

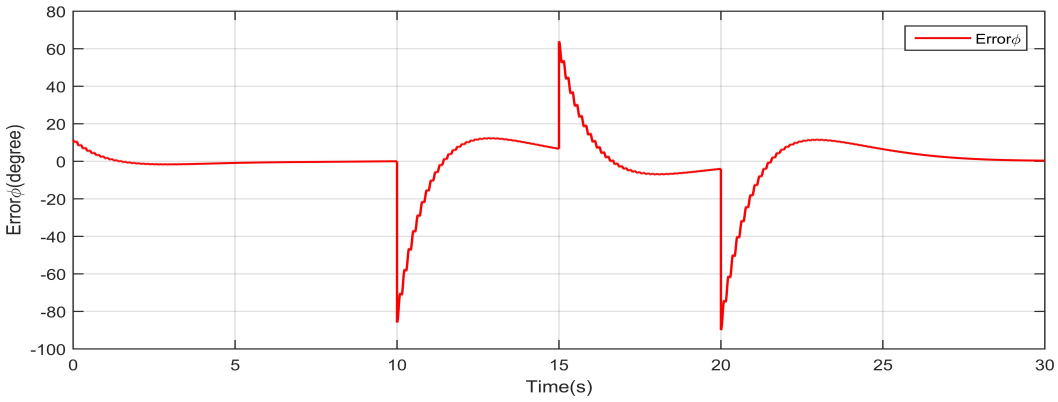

Figure 3.11: Roll error signal evolution(ϕ)

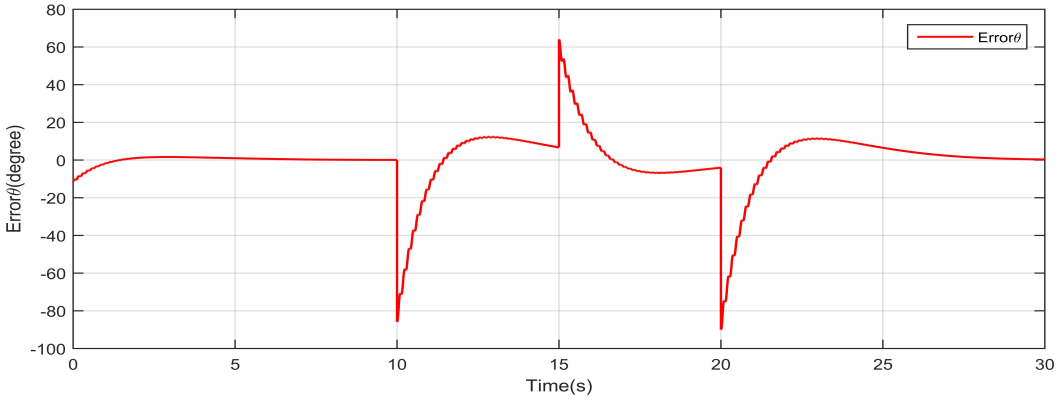

Figure 3.12: Pitch error signal evolution (θ)

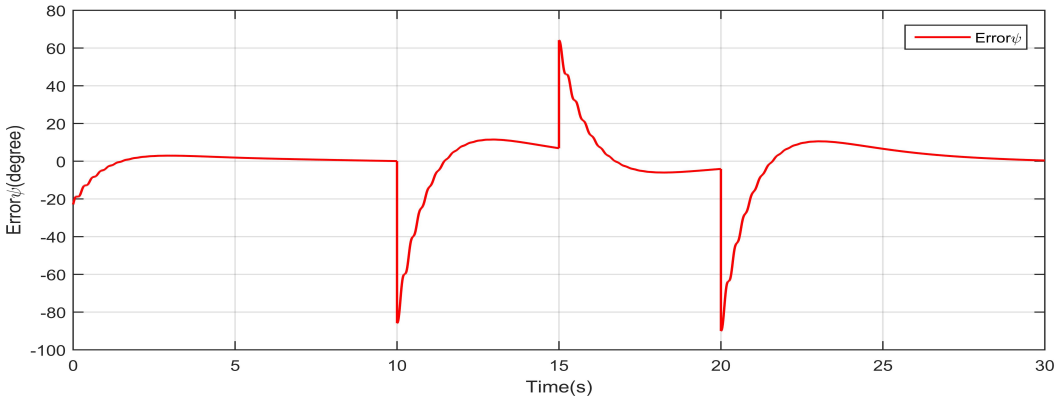

Figure 3.13: Yaw error signal evolution (ψ)

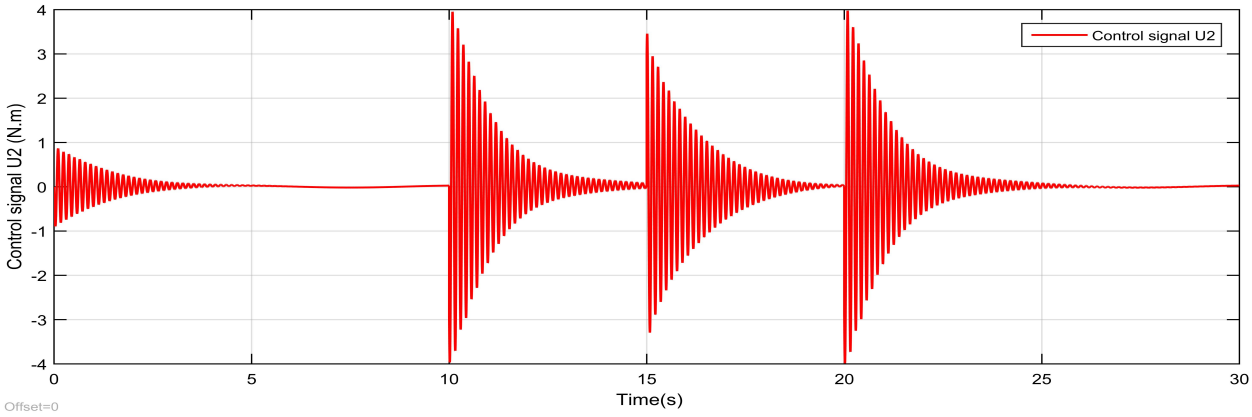

Figure 3.14: graphic curve of control signal U2

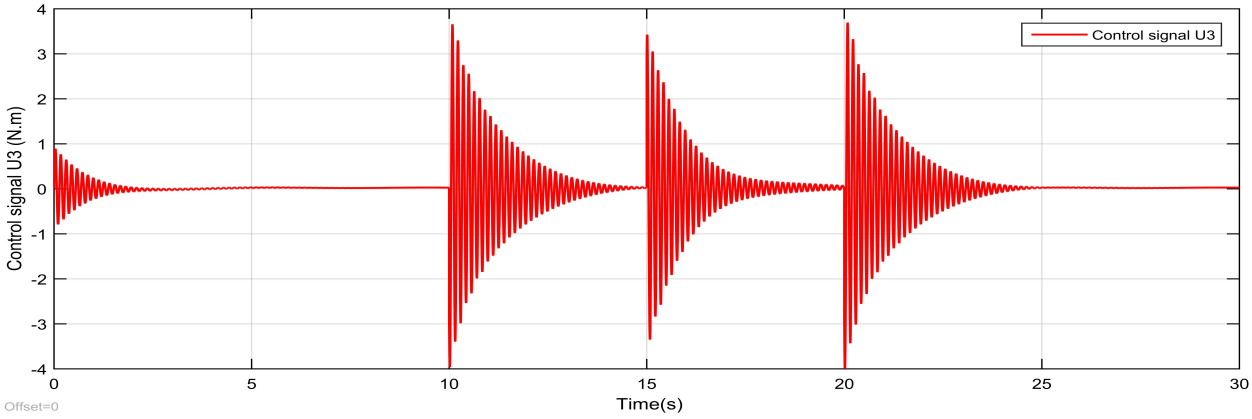

Figure 3.15: graphic curve of the control signal U3

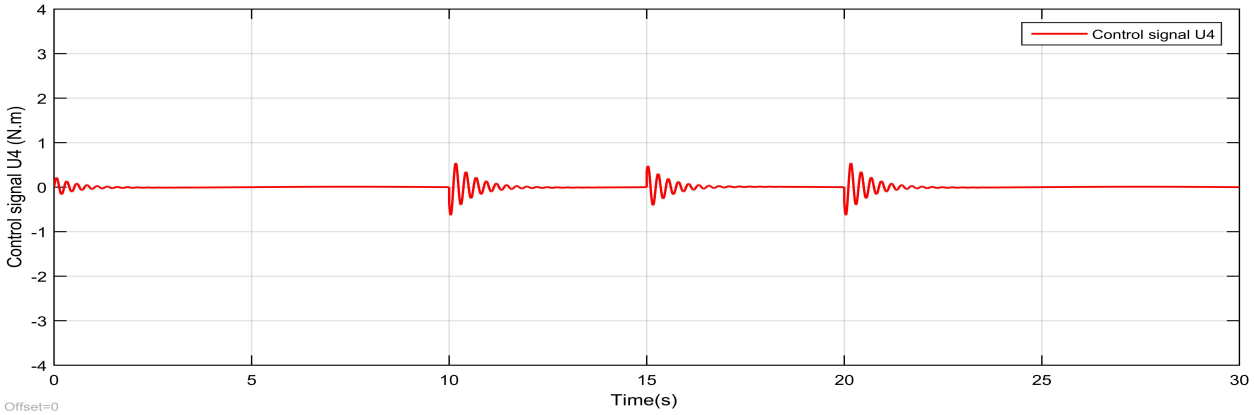

Figure 3.16: graphic curv of the control signal U4

3.3 Synergetic control

3.3.1 A brief review of SC

Consider the following nonlinear system of dimension n:

$$\frac{dx}{dt} = f(x, u, t) \tag{3.7}$$

Or x is the vector of the system state variable, u is the control vector and t is the time. A controller, which produces the control vector u, is used to force the system to operate in the desired way. Synergetic Controller Synthesis starts by defining a macro variable as [25] (please refer to [21] [22] [23] for more details):

$$\varphi = \varphi(x, t) \tag{3.8}$$

Or φ is the macro-variable and $\varphi(x, t)$ is a user-defined function of system state variables. Theoretically, the macrovariable can be chosen as some combination of the system state variables. The purpose of the Synergetic Controller is to drive the system to operate on the surface $\varphi = 0$ The macro-variables evolve according to the following equation:

$$T\frac{d\varphi}{dt} + \varphi = 0 \tag{3.9}$$

Or T is the controller parameter that represents the time necessary for the macro-variables to converge to zero. From equations (3.7)-(3.9), we can deduce the following equation:

$$T\frac{\partial\varphi(x, t)}{\partial x} f(x, u, t) + \varphi(x, t) = 0 \tag{3.10}$$

By solving equation (3.9) for u, the control law can be found as:

$$u = g(x, t, \varphi(x, t), T) \tag{3.11}$$

3.3.2 Design of a SC controller for the Quadcopter system

Based on the SC theory, the following macrovariables are considered:

$$\begin{aligned}\varphi_1 &= \omega_\theta - k_1\left(\theta_d - \theta\right) - d_\theta \\ \varphi_2 &= \omega_\phi - k_2\left(\phi_d - \phi\right) - d_\phi \\ \varphi_3 &= \omega_\psi - k_3\left(\psi_d - \psi\right) - d_\psi\end{aligned} \tag{3.12}$$

Where k_1, k_2, k_3 are positive constants. The macrovariables φ_1, φ_2, and φ_3 are used to ensure that the orientation angles (θ, ϕ, ψ) of the Quadcopter converge to their desired values $(\theta_0, \phi_0, \psi_0)$. The next step is to synthesize a control law that exponentially drives the system to the desired surface $(\varphi = 0)$ with a dynamic evolution of φ, which can be formulated as follows [7]:

$$T\dot{\varphi}_i + \varphi_i = 0, \quad i \in 1, 2, 3 \tag{3.13}$$

Where $T = T^T > 0$ specifies the convergence rate of the system states. The SC law can be computed by solving the system (2.40) with the evolution Eq. (3.13) and the corresponding macrovariables (3.12), resulting in the following outcome:

$$\begin{aligned}u_2 &= \frac{1}{l}\left(\frac{I_x}{T}\left(-\omega_\phi + k_2\left(\phi_d - \phi\right) + d_\phi + Tk_2\left(\dot{\phi}_d - \dot{\phi}\right) + Td_\phi\right) - \omega_\theta\omega_\psi\left(I_y - I_z\right) + J\omega_\theta\Omega - d_\phi\right) \\ u_3 &= \frac{1}{l}\left(\frac{I_y}{T}\left(-\omega_\theta + k_1\left(\theta_d - \theta\right) + d_\theta + Tk_1\left(\dot{\theta}_d - \dot{\theta}\right) + Td_\theta\right) - \omega_\phi\omega_\psi\left(I_z - I_x\right) + J\omega_\phi\Omega - d_\theta\right) \\ u_4 &= \frac{I_z}{T}\left(-\omega_\psi + k_3\left(\psi_d - \psi\right) + d_\psi + Tk_3\left(\dot{\psi}_d - \dot{\psi}\right) + Td_\psi\right) - \omega_\phi\omega_\theta\left(I_x - I_y\right) - d_\psi\end{aligned} \tag{3.14}$$

The following figure shows the structure of the proposed controller.

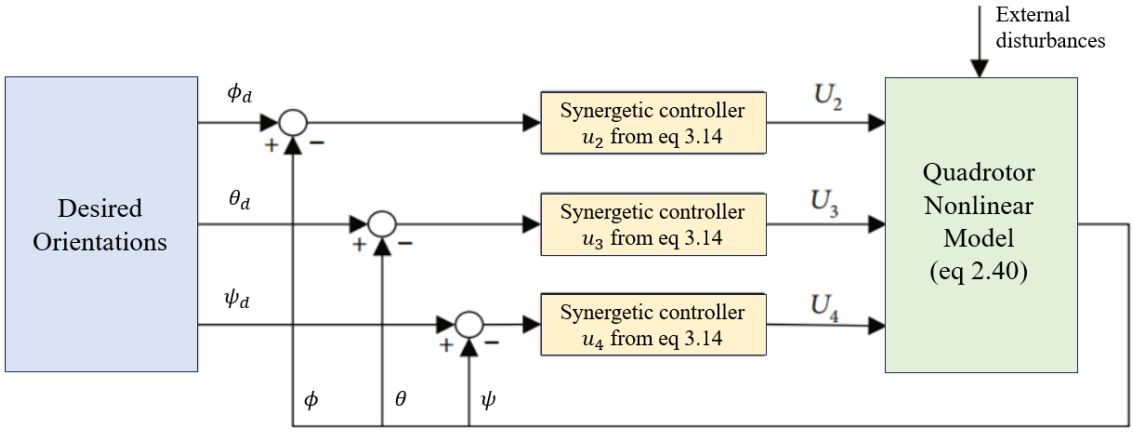

Figure 3.17: Inner and-outer loop of the proposed controller

3.3.2.1 Stability analysis

Theorem 3.1. *The control signals U in Eq. (3.13) ensure the stability of the Quadcopter system and remain within the desired surface.[24]*

Proof. The following Lyapunov function is chosen in terms of macro-variables:

$$V = \frac{1}{2}\left(\varphi_1^T\varphi_1 + \varphi_2^T\varphi_2 + \varphi_3^T\varphi_3\right) \tag{3.15}$$

Taking the time derivative of the equation above, we obtain:

$$\dot{V} = \varphi_1^T\dot{\varphi}_1 + \varphi_2^T\dot{\varphi}_2 + \varphi_3^T\dot{\varphi}_3 \tag{3.16}$$

By substituting equation (3.16) into the expression, we have: (3.17)

$$\begin{aligned}\dot{V} =& \varphi_1\left(-\frac{1}{T_1}\varphi_1\right) + \varphi_2\left(-\frac{1}{T_2}\varphi_2\right) + \varphi_3\left(-\frac{1}{T_1}\varphi_3\right)\\ =& -\left[\frac{1}{T_1}\varphi_1^2 + \frac{1}{T_2}\varphi_2^2 + \frac{1}{T_1}\varphi_3^2\right]\end{aligned} \tag{3.17}$$

Therefore, $\dot{V} \leq 0$. Thus, the stability of the Quadcopter system is guaranteed. □

3.3.3 Simulation results

The proposed synergetic control strategy is applied to the Quadcopter orientation problem to verify its effectiveness and performance. The same initial conditions for roll, pitch, and yaw angles used in Section 3.2.3 are considered. It should be noted that the objective of the controller is to ensure that the Quadcopter orientations asymptotically follow the desired angles, while the tracking error converges to zero.

In this simulation, we consider the same reference trajectories used in Section 3.2.3 for the PID control. To compare the robustness between PID and synergetic control, we utilize identical disturbance values as employed in the PID controller case. Specifically, the disturbance values used are $d_\phi = 1.5$ Nm, $d_\theta = 1.5$ Nm, and $d_\psi = 1.5$ Nm. These disturbances are introduced at time instants $t = 10s$, $t = 15s$, and $t = 20s$ respectively. The SC parameters used are: $k_1 = k_2 = k_3 = 20$, $T = diag[1000, 500, 100]$. The purpose of this comparison is to evaluate the performance of the two control strategies in the presence of external disturbances.

Figures 3.18-3.20 illustrates the effectiveness of the control strategies in achieving desired orientations for the Quadcopter. It is observed that a slight drift occurs at the moments when the disturbances are introduced. However, the controller promptly adjusts the Quadcopter's angles to minimize the deviation from the desired values, thereby successfully minimizing the tracking error.

To further analyze the control performance, Figures 3.21-3.26 displays the control signals and tracking errors. It is noteworthy that the control signals applied to the Quadcopter

remain within a low range. This characteristic is of great significance when transitioning from simulation to real-world applications, as it ensures efficient and safe operation.

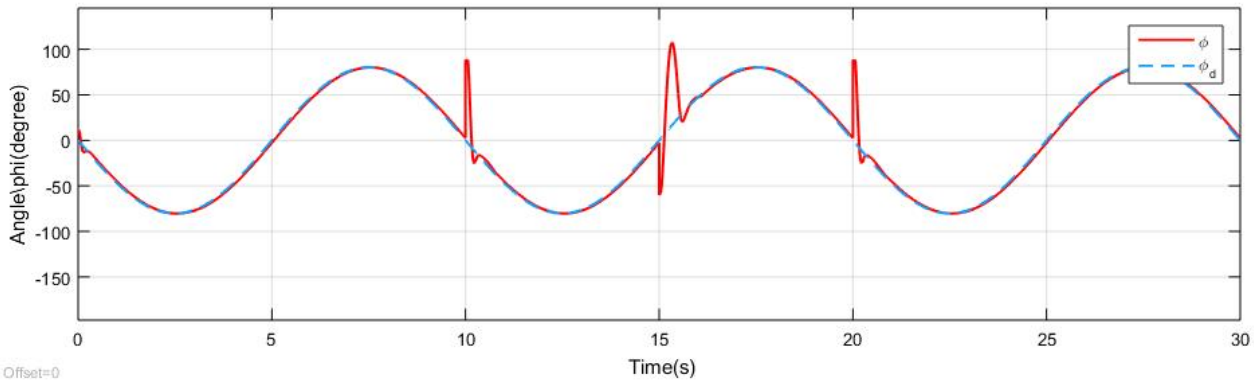

Figure 3.18: graphic curve of the angle ϕ using synergistic control

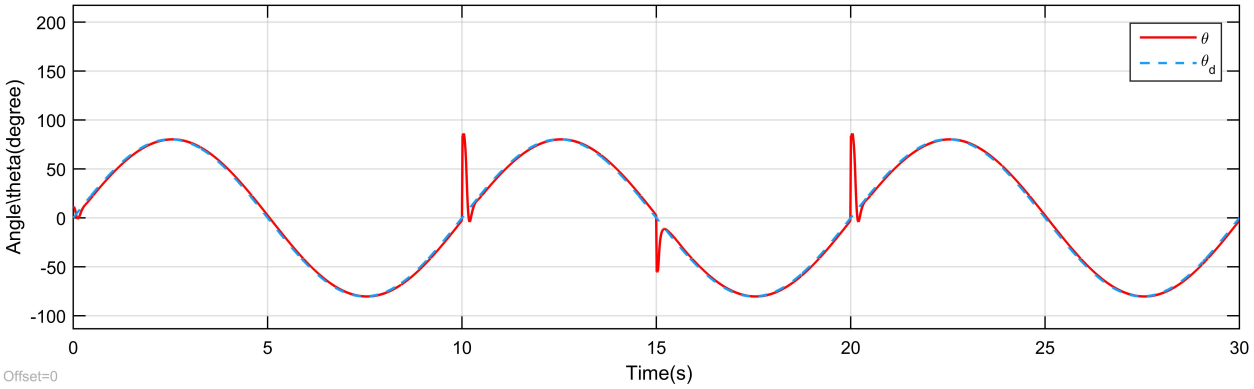

Figure 3.19: graphic curve of the angle θ using synergistic control

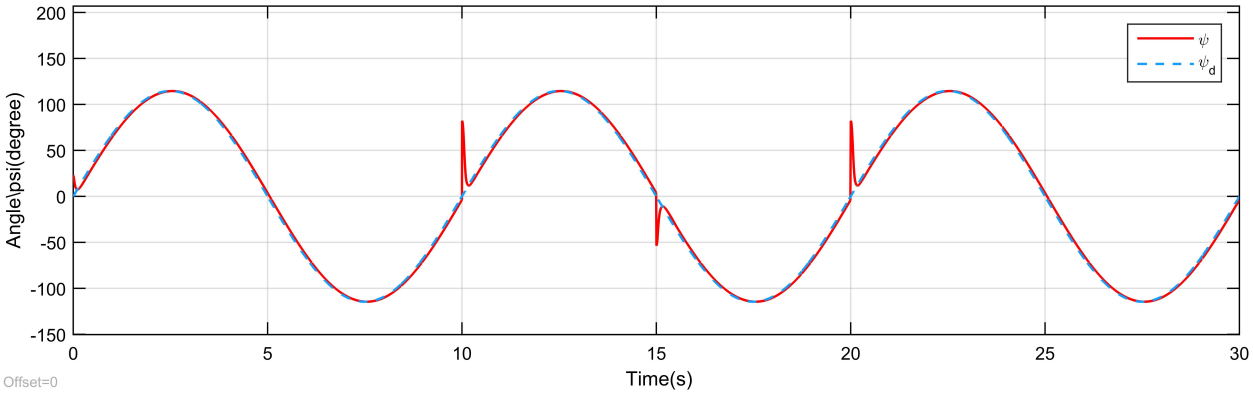

Figure 3.20: graphic curve of the angle ψ using synergistic control

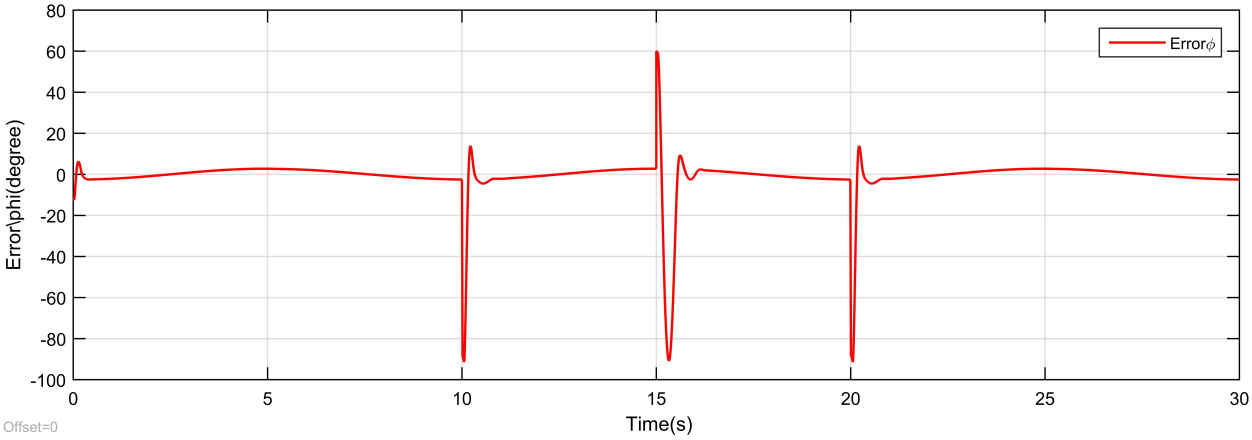

Figure 3.21: graphic curve of the error ϕ using synergistic control

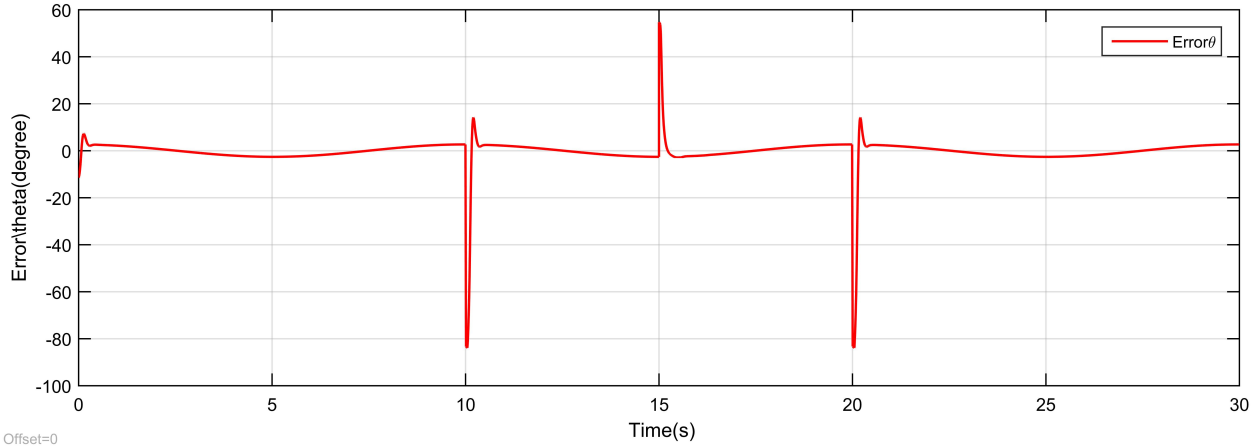

Figure 3.22: graphic curve of the error θ using synergistic control

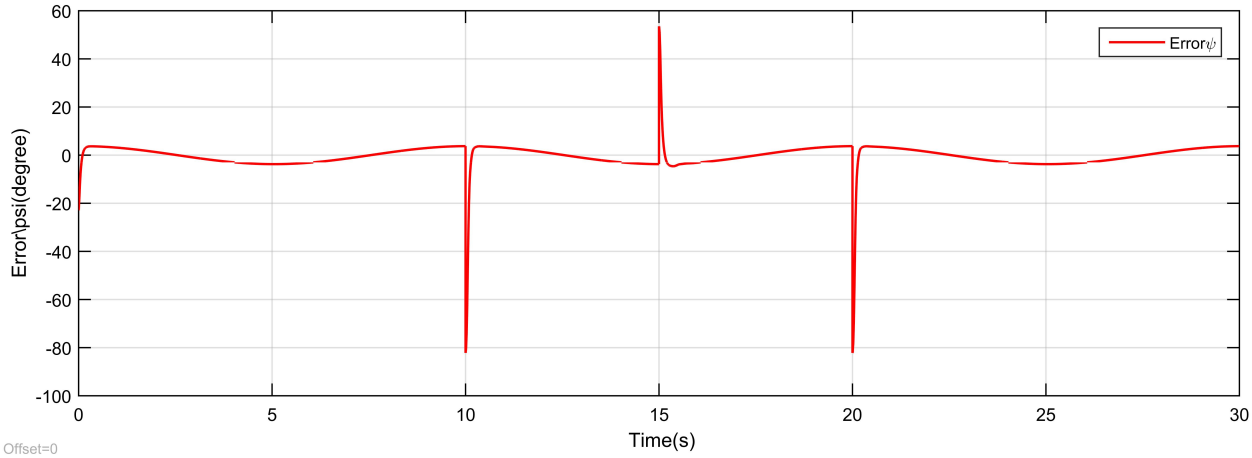

Figure 3.23: graphic curve of the error ψ using synergistic control

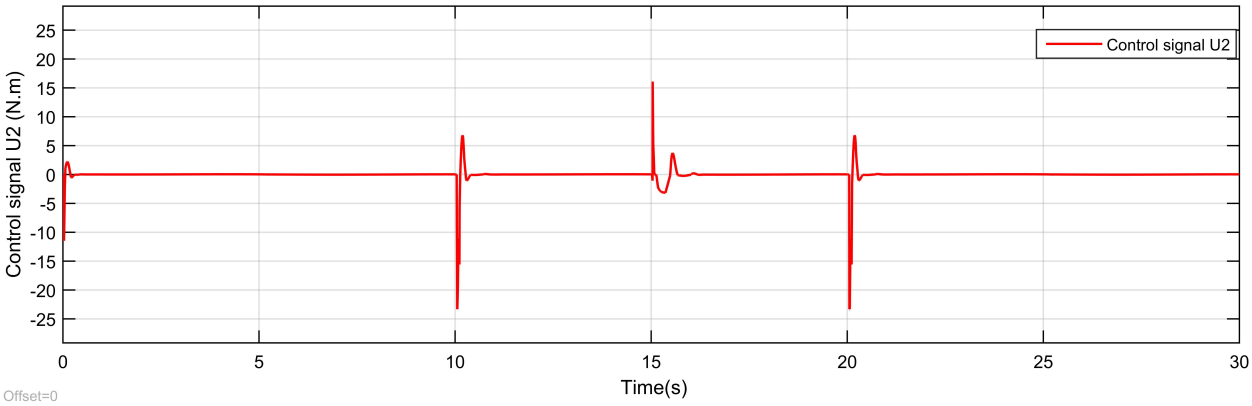

Figure 3.24: graphic curve of the control signal U2 using synergistic control

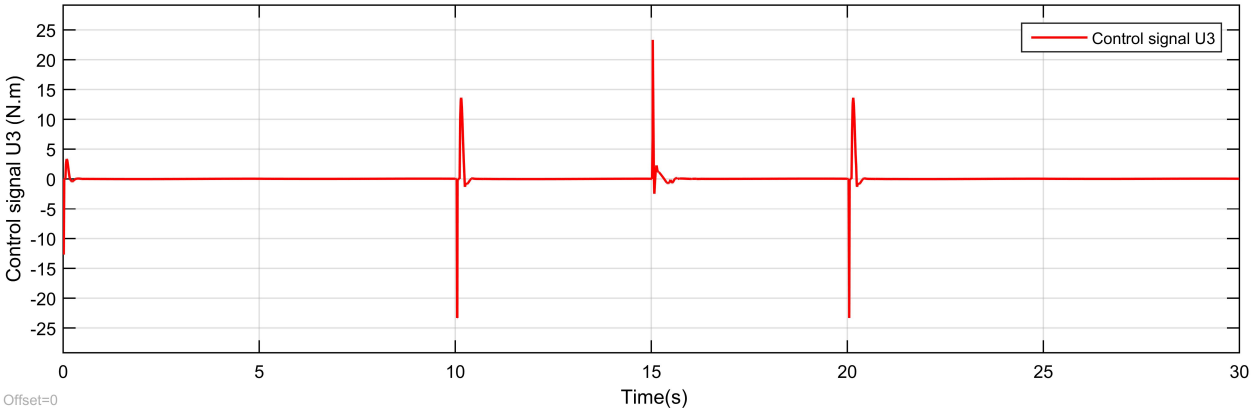

Figure 3.25: graphic curve of the control signal U3 using synergistic control

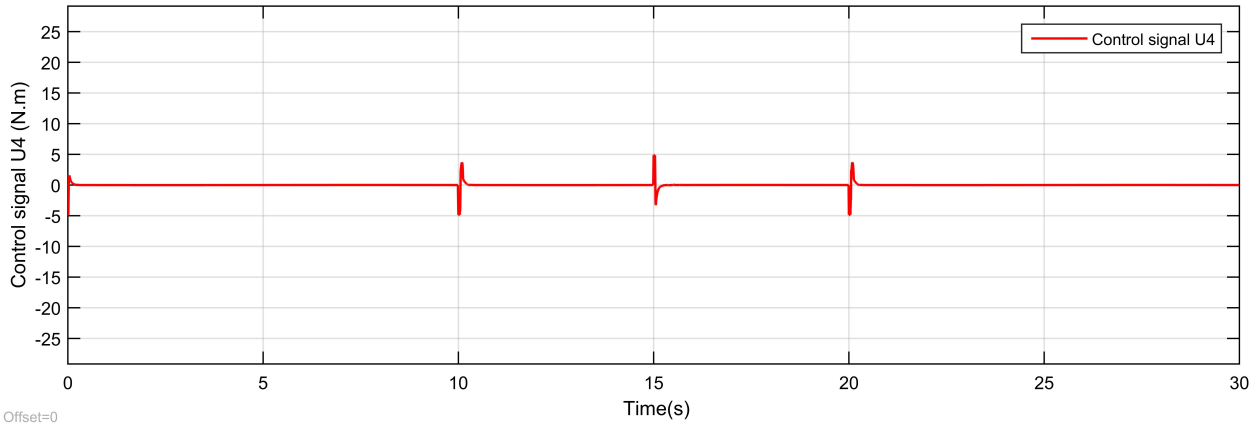

Figure 3.26: graphic curve of the control signal U4 using synergistic control

3.4 Conclusion

In this chapter, we investigate two control strategies for Quadcopter control: the PID controller and the Synergetic controller. Upon examining the results, it became apparent that the synergetic control outperformed the PID controller in terms of error minimization and effectively restoring the angles to their desired values. The synergetic control approach exhibited superior performance by efficiently counteracting the perturbations and rapidly reestablishing the drone's stability.

In comparison, the PID controller displayed larger errors and slower response when confronted with perturbations, requiring more time to bring the angles back to their desired values. This disparity in performance emphasizes the advantage of synergetic control in achieving superior error minimization and control precision under challenging conditions.

In conclusion, the results confirm that the synergetic control approach surpasses the PID controller in terms of error reduction and ensuring the drone's stability, particularly when subjected to perturbations at the specified time instances.

Chapter 4

Experimental validation of the synergetic controllers.

4.1 Introduction

The Quad copter aerial robot stands out as one of the most commonly utilized research platforms for experimental testing. Its widespread popularity can be attributed to its simple structure and cost-effectiveness. Consequently, numerous universities have embarked on designing their own Quadcopters, while open-source projects in this domain are also gaining momentum.

For optimal utilization of such platforms, starting with an open-source project is highly recommended. Leveraging these projects allows researchers to benefit from functional solutions while retaining the flexibility to introduce various modifications at both the hardware and software levels. Among the most renowned open-source hardware and software multirotor projects is the DIY drone project.

The DIY drone project boasts the ArduCopter software, a highly customizable code capable of supporting diverse types of aerial multirotor robots. Complementing the software, the hardware is meticulously developed and made available by 3DR, as showcased in Figure 4.3. The software development closely aligns with hardware advancements, resulting in two autopilot options: the APM2.6 and PixHawk, both adaptable to any platform. To optimize affordability, the combination of a DIY Quadcopter and the Pixhawk autopilot was chosen as the most cost-effective solution. Remarkably, the total hardware cost for this configuration remains below 800 euros. Figure 4.2 visually presents the DIY drone that was meticulously crafted as part of this endeavor.

The present chapter endeavors to introduce the experimental testbed employed, as evidenced in the captivating depiction portrayed in Figure 4.3. This testbed serves as the platform for validating the effectiveness and performance of the proposed PID controller, a pivotal aspect of the thesis at hand.

4.2 Test-bench presentation

The experimental investigations were meticulously conducted based on the comprehensive open-source DIY drone project, encompassing both hardware and software facets. To realize these experiments, a cutting-edge testbed, exemplified in the captivating depiction illustrated in Figure 4.2 , was diligently employed. This purpose-built testbed was meticulously designed to cater to indoor testing requirements, specifically tailored to validate the intricately developed controllers responsible for the precise regulation of Quadcopter attitude.[26]

Within the ambit of this specific experiment, it is crucial to note that, owing to certain technical limitations, our attention was primarily directed towards the roll and pitch movements, thus warranting an in-depth analysis of their dynamics. The testbed dedicated to the meticulous control of attitude boasts a robust stand specifically engineered to provide steadfast support, effectively complemented by the highly versatile and agile DIY Quadcopter. Leveraging advanced technological prowess, the testbed is thoughtfully equipped with a plethora of features aimed at augmenting functionality and ensuring precise and accurate control over the Quadcopter's attitude.

1. Support with rotation ball joint
2. Quad frame
3. Pixhawk autopilot
4. Four electronic speed controllers (ESC)
5. Four brushless motors with propellers
6. Graupner RC receiver
7. 3DR telemetry radios
8. u-blox GPS with compass
9. Power distribution board and LiPo battery
10. APM Power module for current consumption and battery voltage measurement

A seamless RC transmitter plays a crucial role in hardware and software integration, providing manual control and enabling precise command over Quadcopter flight dynamics. Open-source ground control station software, such as QGroundControl or Mission Planner, complements manual control by offering real-time telemetry data visualization, flight mode parameter configuration, and sensor calibration. This comprehensive approach establishes a robust operational framework for Quadcopter experimentation and control. Figure 4.1 visually depicts the meticulous assembly of the Pixhawk 2 autopilot system, showcasing its integration with ancillary components that enhance Quadcopter performance.

The Pixhawk autopilot consists of 32-bit STM32F427 Cortex M4F core, operating at an impressive clock speed of 168 MHz. With 256 KB of RAM and 2 MB of Flash memory, it provides ample computational resources for executing sophisticated algorithms. The system also incorporates a 32-bit STM32F103 failsafe co-processor, adding an extra layer of safety and reliability. For accurate motion sensing and orientation estimation, the Pixhawk integrates a high-performance 6-DoF MPU-6000 accelerometer/gyro, capturing precise acceleration and angular velocity measurements. The inclusion of the ST Micro 3-axis LSM303D accelerometer/magnetometer further enhances the Pixhawk's perception by providing accurate real-time magnetic field measurements. The Pixhawk offers extensive data logging capabilities through a micro SD card slot, facilitating high-rate logging over extended periods. Operating at a frequency of 400 Hz, synchronized with the accelerometer and gyroscope acquisition, the main firmware loop ensures real-time and synchronous data capture, essential for precise control and experimentation.

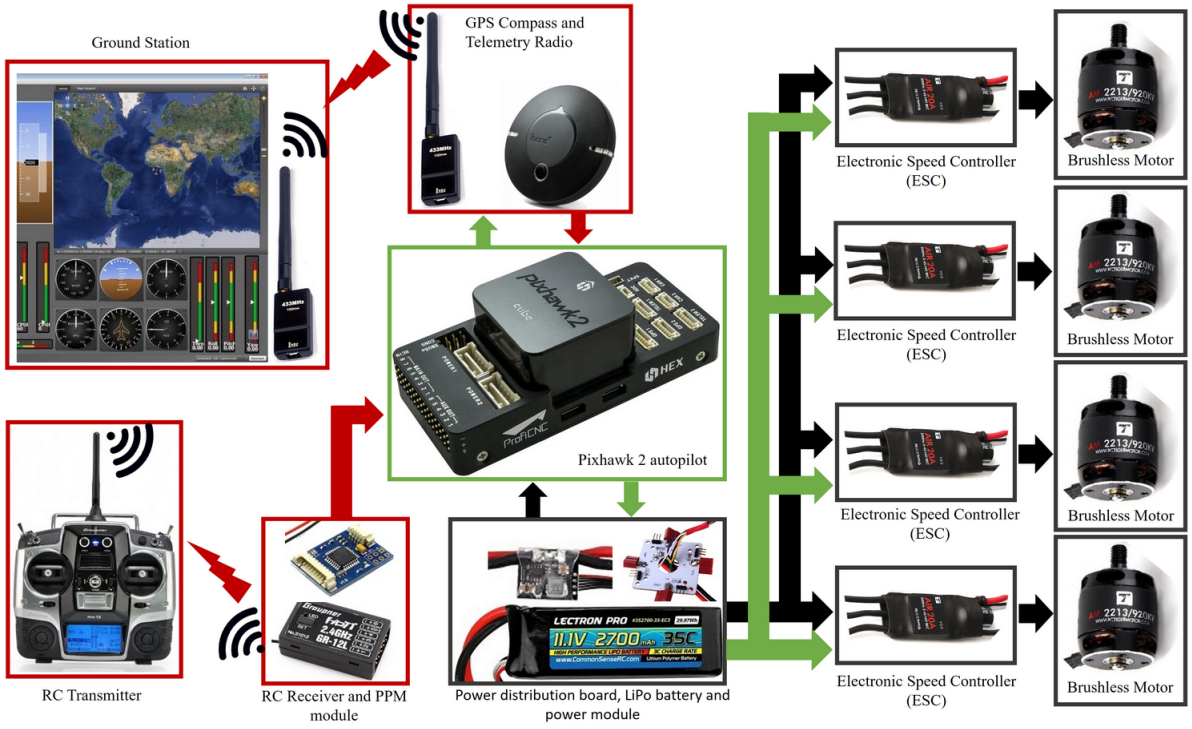

Figure 4.1: Pixhawk 2 mounting [7]

4.3 Experimental validation of the synergetic controller.

Due to some technical issues encountered in this experiment, only the roll and pitch movements are considered. The PID and Synergetic controllers are designed in Matlab/Simulink, utilizing the PX4 support of Embedded Coder. This enables the generation of C/C++ code

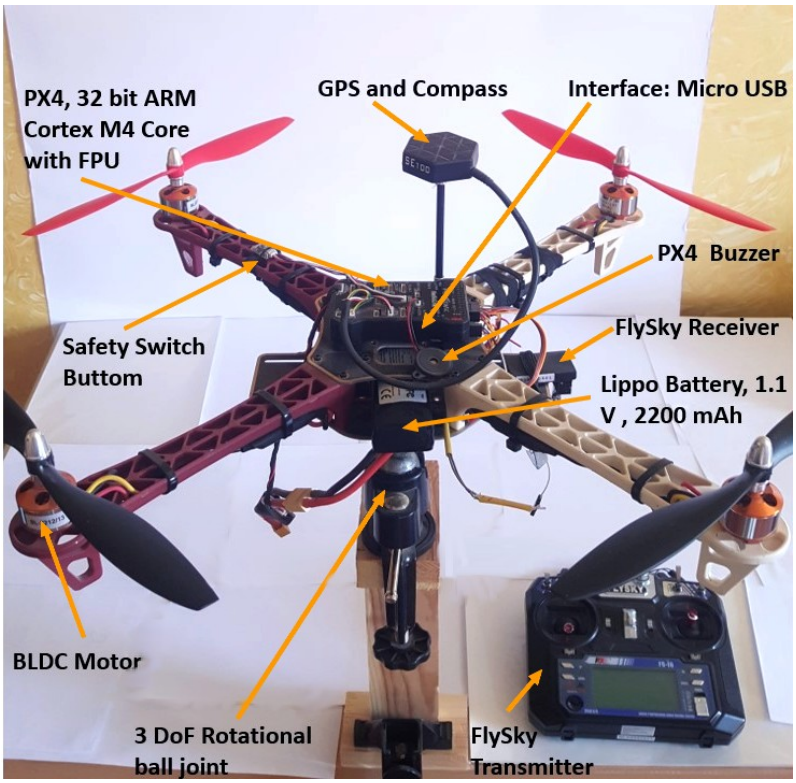

Figure 4.2: Quadcopter test-bench [26]

from Simulink, which can then be deployed onto the microcontroller. The parameters used for the Synergetic control in this experiment are $T = 120, k_2 = 7.5, k_3 = 7.5$.

The experimental results are presented in Figures 4.3 and 4.6. Manual thrust disturbances were introduced at the ends of the Quadcopter arms during the time interval $t \in [3\text{s} - 20\text{s}]$ to demonstrate the ability of the proposed Synergetic controller to handle such disturbances. As shown in Figure 4.3, despite these disturbances, the controller succeeded in maintaining the stability of the Quadcopter. Additionally, the Synergetic controller was subjected to a challenging scenario where a random variable reference was provided by the remote control during the time intervals $t \in [25\text{s} - 45\text{s}]$. A good tracking performance was achieved for the roll and pitch angles, as depicted in Figure 4.3. The tracking error remained relatively low, and once again, the controller only required minimal control effort (as shown in Figure 4.4) to achieve the objective of minimizing the error.

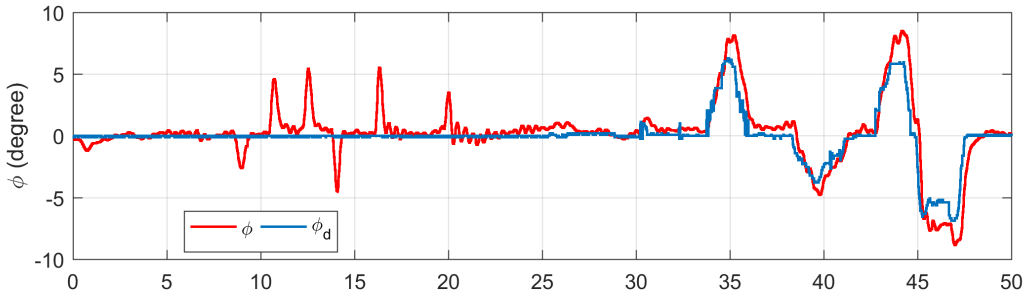

Figure 4.3: graphic curve of the angle ϕ

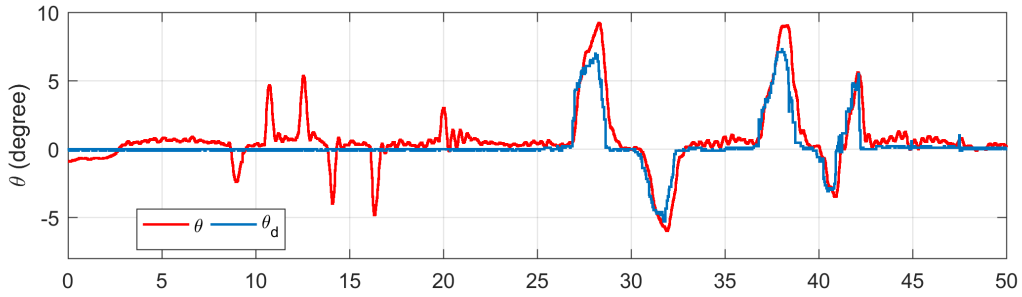

Figure 4.4: graphic curve of the angle θ

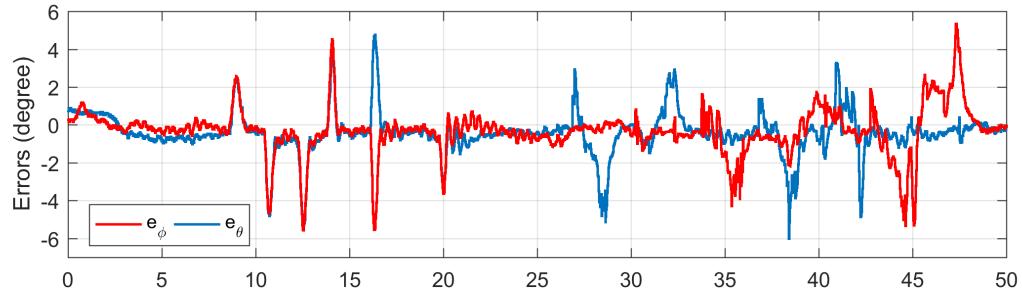

Figure 4.5: graphic curve of the errors θ and ϕ

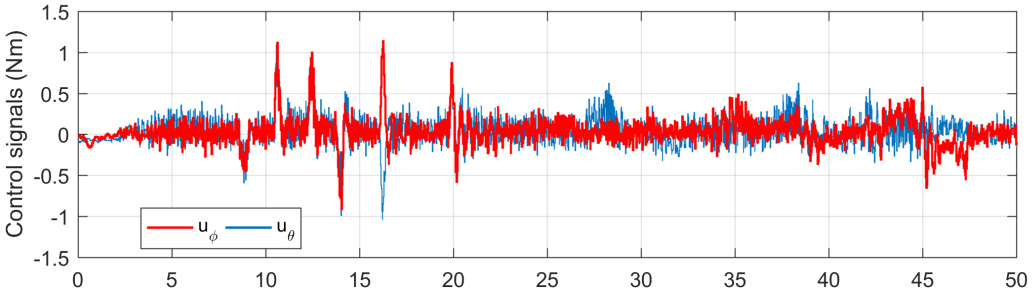

Figure 4.6: graphic curve of the control signals ϕ and θ

4.4 Conclusion

The unmanned aerial vehicle (UAV) markets are experiencing exponential growth, primarily driven by the expanding civilian applications and the high potential of aerial robotics. Typically, using commercial aerial robots for research purposes is challenging, as researchers need to develop their own flight controller to access all the required sensor information and effectively control the robot. This issue is addressed by the emergence of open-source projects in this field. One of the most well-known open-source projects in the aerial robot community is the ArduCopter project. Sponsored by 3DRobotics, the project offers a comprehensive open-source solution for controlling various types of aerial robots. Therefore, we utilized this project as a starting point for conducting experimental research.

The ArduCopter project was modified and successfully used to validate the theoretical research findings. In fact, the proposed control strategy was validated using DIY Quadcopter hardware and the ArduCopter software project. A testbed for attitude control was assembled, incorporating a gimbal mount for safety purposes. The obtained experimental results demonstrate the effectiveness and performance of the proposed controller.

General Conclusion

At the end of this project, we can say that we have delved into a new field of drons and Quad copters so, we have provided an overview of the essential concepts and definitions related to diagnosis based on models and observers. We have identified the fundamental problem of managing the detection and isolation of defects in industrial procedures.

Additionally, we have explored the world of drones, starting with a discussion on their definition and main components. We delved into the history of UAVs and discussed the various classifications of drones, ranging from nano drones to HALE, MALE, mini drones, and micro drones. Furthermore, we focused on quadcopters, highlighting their components, advantages, and diverse applications in both civil and military domains.

The chapter has provided readers with a preliminary understanding of flying robots and their operational principles, with specific emphasis on quadcopters. By utilizing the Newton-Euler formalism, we established the dynamic model of the quadcopter and concluded that it is an underactuated system, characterized by complexity, nonlinearity, and interdependent states.

Moving forward, we introduced two control structures based on PID control and synergetic control. Through experimentation and analysis, we compared the performance of both controllers in terms of minimizing errors and restoring the desired angles (such as ϕ, θ, and ψ) in the presence of perturbations at specific time instances (10s, 15s, and 20s).

The results unequivocally demonstrated the superiority of the synergetic control approach over the PID controller. Synergetic control exhibited enhanced error minimization, quicker response to perturbations, and improved stability restoration. In contrast, the PID controller showcased larger errors and slower response.

Consequently, it can be concluded that synergetic control surpasses PID control in effectively minimizing errors and ensuring the stability of the drone, particularly when confronted with perturbations. These findings underscore the advantages of employing synergetic control techniques in challenging operating conditions for drones.

Bibliography

[1] Paz, R. A. (2001). The design of the PID controller. Klipsch school of Electrical and Computer engineering, 8, 1-23.

[2] Cruz, P. J., & Fierro, R. (2017). Cable-suspended load lifting by a quadrotor UAV: hybrid model, trajectory generation, and control. Autonomous Robots, 41, 1629-1643.

[3] Mátyás, P., & Máté, N. (2019). Brief history of UAV development. Repüléstudományi Közlemények, 31(1), 155-166.

[4] Arjomandi, M., Agostino, S., Mammone, M., Nelson, M., & Zhou, T. (2006). Classification of unmanned aerial vehicles. Report for Mechanical Engineering class, University of Adelaide, Adelaide, Australia, 1-48., year=2006

[5] Aabid, A., Parveez, B., Parveen, N., Khan, S. A., Zayan, J. M., & Shabbir, O. (2022). Reviews on design and development of unmanned aerial vehicle (drone) for different applications. J. Mech. Eng. Res. Dev, 45(2), 53-69.

[6] Ostojic, G., Stankovski, S., Tejic, B., Dukić, N., & Tegeltija, S. (2015). Design, control and application of quadcopter. International Journal of Industrial Engineering and Management, 6(1), 43.

[7] Khalil, Mokhtari. (2021). Multivariable Control of Not Almost Strictly Positive Real Systems (ASPR). PhD thesis, University Ferhat Abbas of Setif 1.

[8]] Astrom, K. and T. Hagglund, (1995) PID Controllers: Theory, Design, and Tuning, 2nd Edition, Instrument Society of America

[9] Panda, R. C. (Ed.). (2012). Introduction to PID controllers: theory, tuning and application to frontier areas. BoD–Books on Demand.

[10] Palm, W. J. (1999). Matlab for engineering applications. WCB/McGraw-Hill.

[11] Knospe, C. R. (2000). PID Control: Tuning and Anti-Windup Techniques. Practical Control Techniques for Control Engineering.

[12] Adigbli, P., Grand, C., Mouret, J. B., & Doncieux, S. (2007). Nonlinear attitude and position control of a micro quadrotor using sliding mode and backstepping techniques. In 7th European Micro Air Vehicle Conference (MAV07) (pp. 1-9).

[13] Bouadi, H., Bouchoucha, M., & Tadjine, M. (2007). Sliding mode control based on backstepping approach for an UAV type-quadrotor. World Academy of Science, Engineering and Technology, 26(5), 22-27.

[14] Bouadi, H., Bouchoucha, M., & Tadjine, M. (2007). Modelling and stabilizing control laws design based on backstepping for an UAV type-quadrotor. IFAC Proceedings Volumes, 40(15), 245-250.

[15] Derafa, L., Madani, T., & Benallegue, A. (2006, December). Dynamic modelling and experimental identification of four rotors helicopter parameters. In 2006 IEEE international conference on industrial technology (pp. 1834-1839). IEEE.

[16] Khebbache, H., Sait, B., Yacef, F., & Soukkou, Y. (2012). Robust stabilization of a quadrotor aerial vehicle in presence of actuator faults. International Journal of Information Technology, Control and Automation, 2(2), 1-13.

[17] Ko, A., Ohanian, O., & Gelhausen, P. (2007, August). Ducted fan UAV modeling and simulation in preliminary design. In AIAA modeling and simulation technologies conference and exhibit (p. 6375).

[18] Kuantama, E., Vesselenyi, T., Dzitac, S., & Tarca, R. (2017). PID and Fuzzy-PID control model for quadcopter attitude with disturbance parameter. International journal of computers communications & control, 12(4), 519-532.

[19] Argentim, L. M., Rezende, W. C., Santos, P. E., & Aguiar, R. A. (2013, May). PID, LQR and LQR-PID on a quadcopter platform. In 2013 International Conference on Informatics, Electronics and Vision (ICIEV) (pp. 1-6). IEEE.

[20] Paiva, E., Soto, J., Salinas, J., & Ipanaqué, W. (2016, October). Modeling, simulation and implementation of a modified PID controller for stabilizing a quadcopter. In 2016 IEEE International Conference on Automatica (ICA-ACCA) (pp. 1-6). IEEE.

[21] Steward, C., & Byl, K. Attitude Tracking of a Quadrotor System through Synergistic Hybrid Feedback Control on SO (3).

[22] Belmouhoub, A., Bouzid, Y., Medjmadj, S., & Siguerdidjane, H. (2022). Robust Control based on Synergetic Theory for Transformable Quadrotor. IFAC-PapersOnLine, 55(22), 31-36.

[23] Steward, C., & Byl, K. Attitude Tracking of a Quadrotor System through Synergistic Hybrid Feedback Control on SO (3).

[24] Alfuqaha, M., Fareh, R., Sinan, S., & Bettayeb, M. (2021, December). Tracking Control of Quadcopter Based on Multiple Manifold of Synergetic Control Strategy. In 2021 14th International Conference on Developments in eSystems Engineering (DeSE) (pp. 186-191). IEEE.

[25] A. A. Kolesnikov, "Introduction of synergetic control", 2014 American Control Conference, pp. 3013-3016, 2014.

[26] Abdessemed Yassine, Srairi Fawzi, Mokhtari Khalil, et al. A robust synergetic controller for quadrotor obstacle avoidance using bezier curve versus b-spline trajectory generation. Intelligent Service Robotics, 15(1):143–152, 2022. 42